NAVAL POSTGRADUATE SCHOOL

MONTEREY, CALIFORNIA

THESIS

HIGH POWER OPTICAL CAVITY DESIGN AND CONCEPT OF OPERATIONS FOR A SHIPBOARD FREE ELECTRON LASER WEAPON SYSTEM

by

Timothy S. Fontana

December 2003

Thesis Advisor: William B. Coulson
Second Reader: Robert L. Armstead

Approved for Public Release; Distribution Unlimited

THIS PAGE INTENTIONALLY LEFT BLANK

REPORT DOCUMENTATION PAGE			Form Approved OMB No. 0704-0188
Public reporting burden for this collection of information is estimated to average 1 hour per response, including the time for reviewing instruction, searching existing data sources, gathering and maintaining the data needed, and completing and reviewing the collection of information. Send comments regarding this burden estimate or any other aspect of this collection of information, including suggestions for reducing this burden, to Washington headquarters Services, Directorate for Information Operations and Reports, 1215 Jefferson Davis Highway, Suite 1204, Arlington, VA 22202-4302, and to the Office of Management and Budget, Paperwork Reduction Project (0704-0188) Washington DC 20503.			
1. AGENCY USE ONLY *(Leave blank)*	**2. REPORT DATE** December 2003	**3. REPORT TYPE AND DATES COVERED** Master's Thesis	
4. TITLE AND SUBTITLE: High Power Optical Cavity Design and Concept of Operations for a Shipboard Free Electron Laser Weapon System			**5. FUNDING NUMBERS**
6. AUTHOR(S) LT Timothy S. Fontana, USN			
7. PERFORMING ORGANIZATION NAME(S) AND ADDRESS(ES) Naval Postgraduate School Monterey, CA 93943-5000			**8. PERFORMING ORGANIZATION REPORT NUMBER**
9. SPONSORING /MONITORING AGENCY NAME(S) AND ADDRESS(ES) N/A			**10. SPONSORING/MONITORING AGENCY REPORT NUMBER**
11. SUPPLEMENTARY NOTES The views expressed in this thesis are those of the author and do not reflect the official policy or position of the Department of Defense or the U.S. Government.			
12a. DISTRIBUTION / AVAILABILITY STATEMENT Approved for Public Release; Distribution Unlimited			**12b. DISTRIBUTION CODE**

13. ABSTRACT ***(maximum 200 words)***

A megawatt (MW)class Free Electron Laser (FEL) as a point defense weapon system may lead to a revolution in anti-ship missile defense. Deep magazine, low cost per shot, proportional engagement capability, and speed of light energy delivery provide the FEL with unmatched advantages over kinetic energy weapon systems. Before an FEL is made fleet deployable, stability, system parameter optimization, and operational utility all must be taken into account.

A short Rayleigh length FEL design is being considered in order to reduce system size and mitigate resonator mirror damage. A short Rayleigh length though can lead to vibrational sensitivities which must be studied. This thesis demonstrates that utilizing currently available technology and properly defined parameters, a short Rayleigh length FEL should be able to achieve a MW of power.

This thesis will also establish the viability of the FEL as a fleet deployable point defense weapon system through the development of a Concept of Operations (CONOPS) which draws from current naval warfare doctrine.

14. SUBJECT TERMS FEL, Free Electron Laser, Short Rayleigh Length			**15. NUMBER OF PAGES** 94
			16. PRICE CODE
17. SECURITY CLASSIFICATION OF REPORT Unclassified	**18. SECURITY CLASSIFICATION OF THIS PAGE** Unclassified	**19. SECURITY CLASSIFICATION OF ABSTRACT** Unclassified	**20. LIMITATION OF ABSTRACT** UL

NSN 7540-01-280-5500 Standard Form 298 (Rev. 2-89)
Prescribed by ANSI Std. 239-18

THIS PAGE INTENTIONALLY LEFT BLANK

Approved for Public Release; Distribution Unlimited

HIGH POWER OPTICAL CAVITY DESIGN AND CONCEPT OF OPERATIONS FOR A SHIPBOARD FREE ELECTRON LASER WEAPON SYSTEM

Timothy S. Fontana
Lieutenant, United States Navy
B.S., United States Naval Academy, 1996

Submitted in partial fulfillment of the
requirements for the degree of

MASTER OF SCIENCE IN APPLIED PHYSICS

from the

NAVAL POSTGRADUATE SCHOOL
December 2003

Author: Timothy S. Fontana

Approved by: William B. Colson
Thesis Advisor

Robert L. Armstead
Co-Advisor

James Luscombe
Chairman, Department of Physics

THIS PAGE INTENTIONALLY LEFT BLANK

ABSTRACT

A megawatt (MW) class Free Electron Laser (FEL) as a point defense weapon system may lead to a revolution in anti-ship missile defense. Deep magazine, low cost per shot, proportional engagement capability, and speed of light energy delivery provide the FEL with unmatched advantages over kinetic energy weapon systems. Before and FEL is made fleet deployable, stability, system parameter optimization, and operational utility all must be taken into account.

A short Rayleigh length FEL design is being considered in order to reduce system size and mitigate resonator mirror damage. However, a short Rayleigh length can lead to vibrational sensitivities which must be studied. This thesis demonstrates that utilizing currently available technology and properly defined parameters, a short Rayleigh length FEL should be able to achieve a MW of power.

This thesis will also establish the viability of the FEL as a fleet deployable point defense weapon system through the development of a Concept of Operations (CONOPS) which draws from current naval warfare doctrine.

THIS PAGE INTENTIONALLY LEFT BLANK

TABLE OF CONTENTS

I. INTRODUCTION....1

II. DETAILED DESCRIPTION OF A FREE ELECTRON LASER....3
- A. ELECTRON BEAM SYSTEM....3
  - 1. Photoinjector....4
  - 2. Linear Accelerator....5
  - 3. Beam Pipe....6
  - 4. Undulator....8
  - 5. Beam Dump....9
  - 6. Beam Energy....10
- B. OPTICAL BEAM GENERATION AND CONTROL SYSTEM....10
  - 1. Undulator....11
  - 2. Resonator Cavity....11
  - 3. Optical Beam Pipe....12
  - 4. Beam Director....12
- C. AUXILIARY SYSTEM....13
  - 1. Power....13
  - 2. Cooling....13
  - 3. Vibration Control....14
  - 4. Shielding....14

III. FREE ELECTRON LASER THEORY....17
- A. RESONANCE....17
- B. ELECTRON MOTION....19
  - 1. Pendulum Equation....19
- C. OPTICAL WAVE EQUATION....22
- D. GAIN....24
- E. PHASE SPACE....25

IV. SIMULATIONS OF HIGH-POWER FREE ELECTRON LASERS WITH STRONGLY FOCUSED ELECTRON AND OPTICAL BEAMS....29
- A. INTRODUCTION....29
  - 1. Short Rayleigh Length....29
  - 2. High Power FEL Parameters....30
- B. THREE DIMENSIONAL COMPUTER SIMULATIONS....31
  - 1. Simulation Methods....33
  - 2. Simulation Output Format....34
  - 3. Simulation Results....36
    - *a. Electron Beam Shift....36*
    - *b. Electron Beam Focusing....39*
  - 4. Conclusion....40

V. MULTIMODE SIMULATIONS OF A SHORT-RAYLEIGH LENGTH FEL....41

A. INTRODUCTION....41
1. High Power FEL Parameters....41
B. SIMULATION RESULTS....42
1. Variation of Undulator Periods....42
2. Variation of Electron Beam Waist Radius....43
3. Variation of Normalized Rayleigh Length....44
C. CONCLUSION....45
VI. FEL CONCEPT OF OPERATIONS FOR NAVAL PLATFORMS....47
A. INTRODUCTION....47
B. SYSTEM INTEGRATION....47
1. General Characteristics....47
2. Mission....48
3. Weapons Posture....49
a. Safety Mechanisms....52
4. Watchstanders....53
5. Detect to Engage Sequence....55
C. ENGAGEMENT OPTIONS....56
1. Detection, Tracking, and Fire Control....56
2. Manual Engagements....57
3. Automatic Engagements....58
4. Proportional Engagements....59
D. TACTICS....60
1. Point Defense....60
2. Naval Surface Fire Support....60
3. Anti-Satellite (ASAT)....61
4. Guarded Unit State....61
E. CONOPS SCENARIO (STREAM RAID)....62
1. Geopolitical Situation....62
2. Event Timeline....63
3. Conclusion....68
VII. CONCLUSION....69
LIST OF REFERENCES....71
INITIAL DISTRIBUTION LIST....73

LIST OF FIGURES

Figure 1. This color-coded schematic of an FEL delineates primary functional systems by color. Red is the Electron Beam systems, blue is the optical beam generation and control system, and green is the auxiliary system. The undulator is marked in purple because it is an overlap component between electrons and light. 3
Figure 2. DC Photoinjector. 4
Figure 3. SRF Photoinjector. 4
Figure 4. Superconducting radio frequency cavities within a linear accelerator. SRF cavities can achieve an acceleration gradient of 18MV/m under proper conditions. The LINAC is made of multiple SRF cavities. Each cavity consists of 5 to 7 individual cells. 6
Figure 5. Quadrupole. Quadrupole magnets are used to "funnel" the electron beam down the longitudinal axis of the beam pipe and avoid scraping. The arrows initiated within the magnets indicate the direction of the magnetic field. 7
Figure 6. Undulator. Inside the undulator, an alternating magnetic field causes the relativistic electron beam to "wiggle", which causes the electrons to emit radiation. This schematic does not depict the number of undulator periods proposed for the MW class FEL, it merely depicts general undulator design. 8
Figure 7. Conceptual design of an FEL director assembly. 12
Figure 8. Cross-section of a fresh water cooled beam dump. 14
Figure 9. Photon-Electron Race 17
Figure 10. Phase Space Plot for $\nu_o = 0$ 26
Figure 11. Phase Space Plot for $\nu_o = 2.6$ 27
Figure 12. Electron Beam Off-axis Shift 32
Figure 13. Strongly Focused Electron Beam 33
Figure 14. Three Dimensional Simulation Output Format 35
Figure 15. Single Pass Extraction Efficiency versus Initial Phase Velocity for Various Values of the Normalized Beam Shift. 37
Figure 16. Peak Single-Pass Extraction versus the Normalized Electron Beam Shift 38
Figure 17. Peak Single-Pass Extraction and Induced Energy Spread versus Normalized Electron Beam Radius 39
Figure 18. Simulation results for extraction, η, versus number of undulator periods *N*. 42
Figure 19. Simulation results for extraction, η, versus normalized electron beam radius, σ 43
Figure 20. Simulation output file of a weakly-focused electron beam. 44
Figure 21. Simulation output of a strongly-focused electron beam. 44
Figure 22. Simulation results for extraction, η, and mirror intensity versus normalized Rayleigh length, z_o. 45

Figure 23. FEL 360º weapons coverage. 48
Figure 24. Combat Information Center Organization with Directed Energy Weapons Supervisor included. 53
Figure 25. Commanding Officer and Tactical Action Officer Console in DDG 51 Class Guided Missile Destoryers. 54
Figure 26. DTE with incorporated FEL weapon system. 55
Figure 27. Dhow intercepted by USS OSCAR AUSTIN (DDG 79) 63
Figure 28. Strait of Hormuz and South Arabian Gulf. 64
Figure 29. Console view of tactical situation at Time 00:08:00. RESONATOR's VSR has detected missile launches from Siri Island. 65
Figure 30. Console view of tactical situation at Time 00:09:36. Auto engagement doctrine has automatically engaged the inbound threats. Note the range change from 64 NM to 16 NM. 66
Figure 31. Console view of the tactical situation at Time 00:09:51. FEL Director 1 engages the first inbound leaker. Note the range change from 16 NM to 8 NM 67

LIST OF TABLES

Table 1 Undulator Design Parameters. 9
Table 2 Optical Resonator Cavity Parameters for a MW-Class FEL (From [Ref. 3]) 30
Table 3 Undulator parameters for MW-Class FEL (From [Ref. 3]) 31
Table 4 Electron beam parameters for a MW-Class FEL (From [Ref. 3]) 31
Table 5 Weapons Postures for an FEL....51

THIS PAGE INTENTIONALLY LEFT BLANK

ACKNOWLEDGMENTS

First and foremost I would like to thank my parents for their unconditional support, charity, and love throughout my naval career and my life. Without your advice and understanding I would never have become the student, Naval Officer, and Father I am today. Thank you so very much. Never in a thousand lifetimes could I ever repay you for everything you have given me.

To Professor Colson and the rest of the FEL Professors, thank you for your endearing patience and your bottomless travel coffers. The undebateable vastness of your knowledge is truly astounding. Thank you for working so hard to impart simply a fraction of it upon the slippery slope that is my brain.

To the boys in the office, I would need a hundred pages to reminisce about our times spent together in the office and abroad and to thank you for all the support, friendship, and homework assignm,…err, I mean academic assistance you have given me over the past few years. I never would have graduated without you all, and I almost didn't because of you all. I hope you know that I received no greater reward while here at NPS than your friendship and camaraderie. Thank you.

Most importantly though, I want to thank my little partner, Joshua, and my perfect princess, Katelyn. I know it will be years before you fully comprehend our experience in Monterey. Please know that my love for you is the driving force in my life. I love and cherish you with more passion than I though humanly possible. I have dedicated my life to showing you exactly how precious you are to me and to ensure that you know that I will always be your Daddy.

THIS PAGE INTENTIONALLY LEFT BLANK

LIST OF ACRONYMS

Acronym	Definition
MW	Megawatt
FEL	Free Electron Laser
CONOPS	Concept of Operations
ASCM	Anti-Ship Cruise Missile
NSFS	Naval Surface Fire Support
DEW	Directed Energy Weapon
HEL	High Energy Laser
ASAT	Anti-Satellite
LINAC	Linear Accelerator
RF	Radio Frequency
SRF	Superconducting Radio Frequency
IPS	Integrated Power System
DDG	Guided Missile Destroyer
NM	Nautical Mile
LSF	Low Slow Flyer
LOS	Line of Sight
UAV	Unmanned Aerial Vehicle
WP	Weapons Posture
VLS	Vertical Launch System
SM	Standard Missile

DEWS	Directed Energy Weapons Supervisor
DLC	Drive Laser Cutoff
CIC	Combat Information Center
RFFC	Radio Frequency Field Cutoff
TAO	Tactical Action Officer
AIR	Air Warfare Coordinator
CO	Commanding Officer
MSS	Missile Systems Supervisor
SUWC	Surface Warfare Coordinator
FC	Fire Controlman
NEC	Naval Education Code
ST	Sonar Technician
DTE	Detect to Engage
VSR	Volume Search Radar
ROE	Rules of Engagement
FCS	Fire Control System
BDA	Battle Damage Assessment
VAB	Variable Action Button
MOVE	Manually Observed Verified Engagement
AWS	Aegis Weapon System
PD	Point Defense
UNREP	Underway Replenishment
GUS	Guarded Unit State

UN	United Nations
SAG	Southern Arabian Gulf
MIO	Maritime Interception Operations
NAG	Northern Arabian Gulf
SSES	Ships Signal Exploitation Space
BZ	Bravo Zulu (Warfare Commander)

THIS PAGE INTENTIONALLY LEFT BLANK

I. INTRODUCTION

Recent technological advances have produced a series of high speed, low altitude, rapid maneuvering anti-ship cruise missiles (ASCM) which pose a serious threat to the U.S. Navy around the world. Cold war era weapon systems currently deployed are stretched to the limit of their capabilities to defend against such threats. Ideally, what is required to defend against these new threats is a weapon system that can hit the intended target with sufficient energy to kill it, but also fast enough to negate any offensive advantages such as those listed above. It should also be able to disable any target within sight, perform multiple missions, and maintain a low cost per engagement.

Kinetic energy weapon systems are unable to fulfill the above listed idealized requirements. Guns and missiles have limited speed and lethality; they can miss their targets or even hit them and fail to kill them. Actually achieving a hit is extremely difficult for such systems because the target can move while the gun projectile or missile is in flight, and forces such as gravity and air resistance can deflect the weapon from the proper course. Many current naval weapon systems are capable of only fulfilling a single mission area, such as air defense, or Naval Surface Fire Support (NSFS). Those systems which are multi-mission capable can only do so at a reduced capacity.

Directed energy weapons (DEW) could provide the crucial step in the realization of a significantly improved defensive weapon system. A high energy laser (HEL) could engage potential targets at the speed of light, erasing high speed maneuvering benefits thus giving the advantage back to the defender. Megawatt (MW) level optical beam power would be sufficient to successfully disable nearly any threat in a matter of seconds. While initially expensive to research and manufacture, HEL systems would cost on the order of dollars per engagement as compared to the thousands to hundred of thousands of dollars per engagement of current defensive systems, not to mention the shipboard space saving without the requirement for large projectile storage magazines. Additionally, HEL's could be utilized in multiple mission areas such as point defense, limited area defense, NSFS, and anti-satellite (ASAT) warfare.

For the U.S. Navy, the Free Electron Laser (FEL) is the HEL system of choice for shipboard applications. High power, simple design, tunable wavelength, deep magazine,

small topside footprint and low cost per shot are all advantages of the FEL. The FEL is theoretically capable of achieving more than the MW of output power required to be effective as a naval point defense weapon system. Such an immense power requirement necessitates the use of a short Rayleigh length design to avoid the damaging effects of this intense power on internal optical systems. Certain aspects of such a design are presented in this thesis, specifically high power optical cavity design through the use of computer simulations. Additionally, this thesis will address the Navy's use of an FEL as a point defense weapon system through the development of an FEL Concept of Operations.

Chapter II discusses the major components of the FEL and a general description of how an FEL operates. The individual components are categorized into three specific functional systems: the electron beam system(discussed in considerable detail), the optical beam generation and control system, and the support or auxiliary system.

Chapter III discusses the theory of operation of a free electron laser and establishes how the electron beam energy is converted into laser light energy.

Chapter IV describes the research results for the proposed 1 MW FEL weapon system design utilizing a short Rayleigh length undulator. The short Rayleigh length option was studied utilizing three-dimensional computer simulations to determine the ramifications of off-axis electron beam shifting due to FEL component vibrations and to study the effects of strongly focused electron and optical beams on system performance.

Chapter V presents research conducted to determine optimal resonator cavity parameters through the use of a three-dimensional, multimode simulation program. Specifically, strongly focused optical and electron beams were used to study the effects of varying electron beam, undulator, and optical cavity parameters.

Chapter VI establishes a brief Concept of Operations (CONOPS) for the FEL as a naval at-sea point defense weapon system. From weapons postures to engagement options, this chapter covers a wide range of operational issues. Additionally, a real-time scenario is included to help solidify CONOPS issues discussion and understand the utility of an FEL as a shipboard system.

Chapter VII summarizes the results found in the present study.

II. DETAILED DESCRIPTION OF A FREE ELECTRON LASER

The Free Electron Laser consists of 3 primary functional systems: the electron beam system, the optical beam generation and control system, and the support or auxiliary system, as shown in Figure 1. Each must work in conjunction with others in the system in order to produce the intended output. One of the most critical of these systems is the electron beam system. The following is a detailed description of the electron beam system, followed by a more spartan explanation of the optical beam and auxiliary systems.

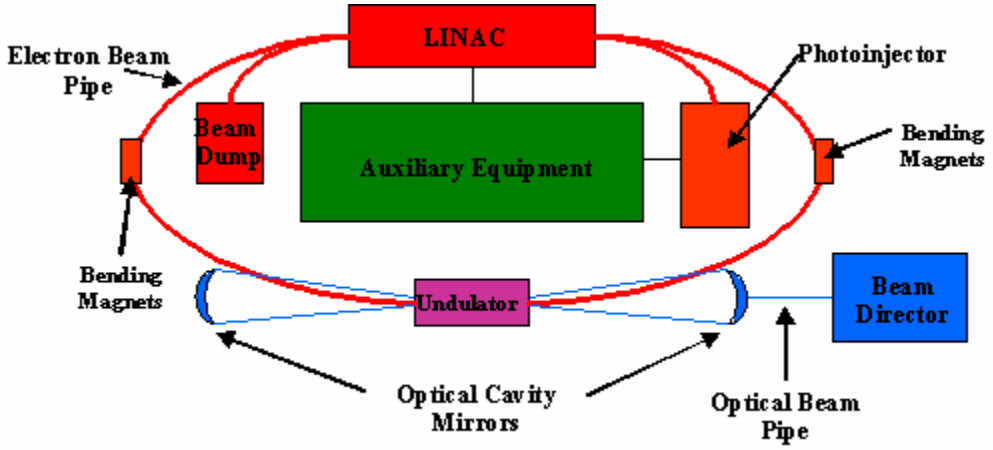

Figure 1. This color-coded schematic of an FEL delineates primary functional systems by color. Red is the Electron Beam systems, blue is the optical beam generation and control system, and green is the auxiliary system. The undulator is marked in purple because it is an overlap component between electrons and light.

A. ELECTRON BEAM SYSTEM

The electron beam system is responsible for the generation, acceleration, transport and disposal of the electron beam. Electron pulse formation and initial acceleration are accomplished within the photoinjector. The beam is then transported directly to the linear accelerator (LINAC) where it is further accelerated to higher energies. This relativistic electron beam is passed through the beam pipe toward the undulator where energy is extracted to create and amplify the outgoing optical beam. The electrons then continue their journey back to the LINAC and enter it 180 degrees out of phase so that the radio frequency (RF) fields extract energy instead of accelerating the electrons. The

result is that most of the beam's energy is recovered, while the remainder is disposed of in the electron beam dump.

1. Photoinjector

The purpose of the photoinjector is to produce high-density electron pulses and inject them into the LINAC for further acceleration. The photoinjector consists of two primary sections: the electron gun and the buncher/accelerator. Figures 2 and 3 depict schematics of two photoinjector designs. Currently Jefferson Laboratory is working on a hybrid DC/Superconducting RF (SRF) photoinjector design that promises low emittance at relatively high charge per bunch[JLAB].

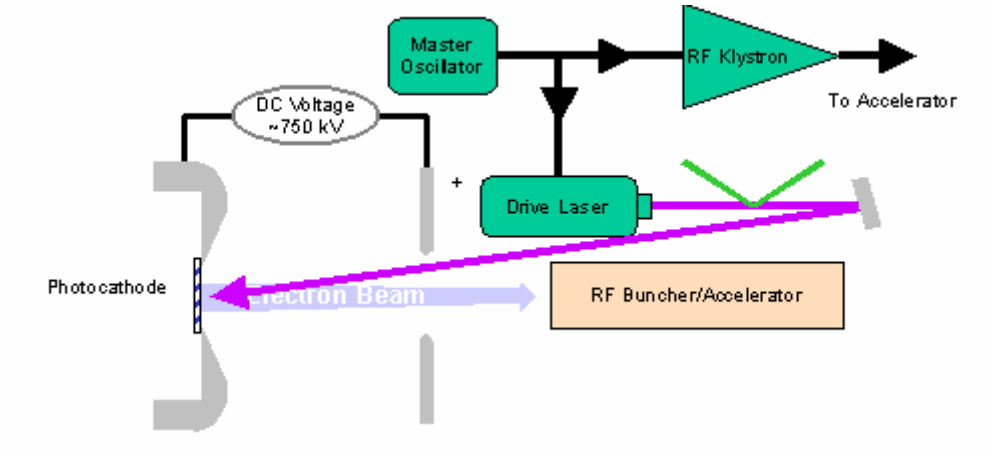

Figure 2. DC Photoinjector.

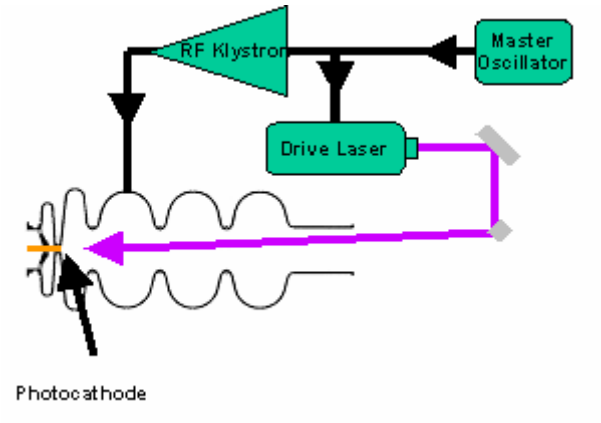

Figure 3. SRF Photoinjector.

The electron gun's primary purpose is to generate electrons. Both designs follow the same principle; a laser focused on a photocathode ejects electrons from the cathode surface through the photoelectric effect. In the DC photoinjector, the ejected electrons are drawn away from the cathode by a high DC voltage and funneled toward the buncher/accelerator. In the superconducting RF (SRF) photoinjector, the expelled electrons immediately enter a single-cell RF focusing cavity, similar to an accelerator cavity. The hybrid system will use a DC high voltage emittance-compensating solenoid to help accelerate the electrons away from the cathode and then transport them to a series of SRF cavities for additional acceleration and bunching [AES]. The hybrid system is the model we will use for the remainder of this chapter.

Once liberated from the cathode, the electrons are accelerated toward the electron buncher/accelerator, in this case the first SRF single cell cavity, where a high voltage RF field bunches the electrons and accelerates the beam to an intermediate energy. The beam then passes through a second SRF accelerating cavity where it achieves a final photoinjector output energy of 7 MeV.

The hybrid photoinjector is designed to operate at a frequency of 750 MHz, an average current of 0.6 A and an output energy of 7 MeV, producing an average power of 4.2 MW. The electrons acquire the remainder of their 110 MeV as they pass through the LINAC.[JLAB]

2. Linear Accelerator

The linear accelerator, or LINAC, is where the electron beam receives the remainder of its energy before it is passed to the undulator. The accelerator is constructed of a number of SRF cavities, Figure 4, which produce an extremely intense oscillating electromagnetic field. This high voltage electromagnetic field runs parallel to the electron acceleration axis and is synchronized with the electron beam pulses generated in the photoinjector so as to increase the electron beam energy to highly relativistic energies. The accelerating gradient is 18 MV/m.

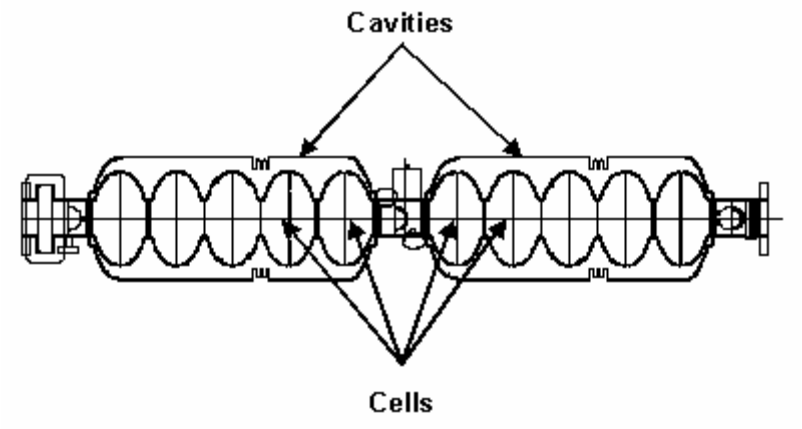

Figure 4. Superconducting radio frequency cavities within a linear accelerator. SRF cavities can achieve an acceleration gradient of 18MV/m under proper conditions. The LINAC is made of multiple SRF cavities. Each cavity consists of 5 to 7 individual cells.

Considering the 103 MeV difference between the photoinjector energy and the LINAC energy, and an acceleration gradient of 18 MV/m, the LINAC would have to be approximately 6 meters in length.

As the electron beam passes through the undulator, a percentage of its energy will be extracted for the creation of the optical beam. The reduced energy electron beam then travels back to the LINAC, but this time the electrons are 180 degrees out of phase relative to the accelerating RF fields. This phase difference causes the electrons to decelerate and transfer their kinetic energy back to RF energy within the LINAC. This energy recovery greatly increases the laser's overall efficiency.

3. Beam Pipe

The "beam pipe" is the general name used to describe the electron transport system, including focusing and bending magnets and the vacuum system.

Imagine an electron beam traveling down the longitudinal axis of a cylindrical steel pipe section. Any interference with the beam as it is transported to the undulator may affect the overall efficiency of the laser. To reduce beam interference, the entire beam pipe, and the entire system for that matter, is kept under a near perfect vacuum. This ensures the beam's unimpeded progress from system to system. The vacuum system itself is part of the auxiliary system.

As shown in Figure 1, the beam does not travel in a straight line from the LINAC to the undulator. Design requirements necessitate that the beam pipe make a series of bends to transport the beam from system to system. Strategically positioned "steering" magnets force the electron beam to follow the curved beam pipe. The magnetic field produced by the steering magnets imparts a magnetic force to the electron beam according to $\vec{F}_{mag} = q(\vec{v} \times \vec{B})$, where q is the electron charge, $\vec{v}$ is the electron velocity, and $\vec{B}$ is the magnetic field[Griffiths]. Since the magnetic field cannot do work on the electrons, there are no significant energy losses from steering the beam.

As the beam travels down the pipe, it must stay centered on the pipe's longitudinal axis. A degradation in laser efficiency and possibly damage to the laser may occur if the electron beam "scrapes" the actual pipe. To avoid scraping the pipe, quadrupole magnets are used to funnel the beam down the longitudinal axis, as shown in Figure 5.

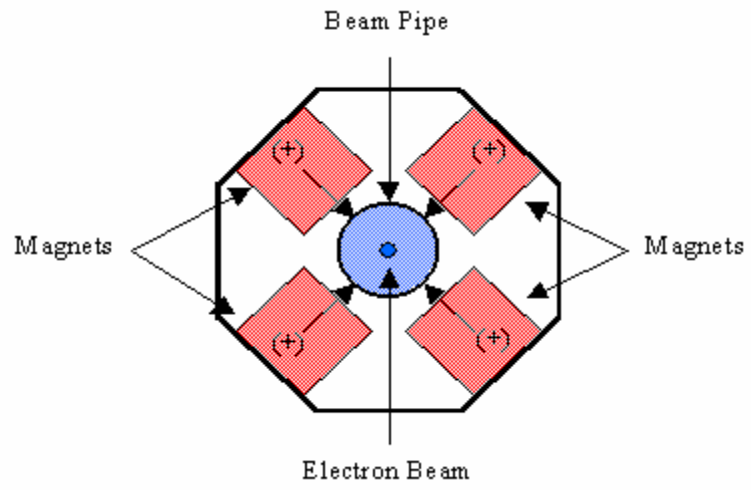

Figure 5. Quadrupole. Quadrupole magnets are used to "funnel" the electron beam down the longitudinal axis of the beam pipe and avoid scraping. The arrows initiated within the magnets indicate the direction of the magnetic field.

The quadrupole consists of 4 magnets with the North end of each pointing inward toward the beam pipe. This configuration establishes the appropriate magnetic field to force the electron beam to the center of the pipe. Quadrupoles are located periodically along the beam pipe to ensure a centralized and focused beam upon entry to major system

components. Sextupoles and octupoles are also used along the beam pipe to serve the same purpose.

4. Undulator

The undulator, or "wiggler," is considered an overlap component between the electron beam system and the optical beam generation and control system, and therefore will be covered both in this subsection and the next on the optical beam generation and control system. Figure 6 depicts a simple undulator schematic.

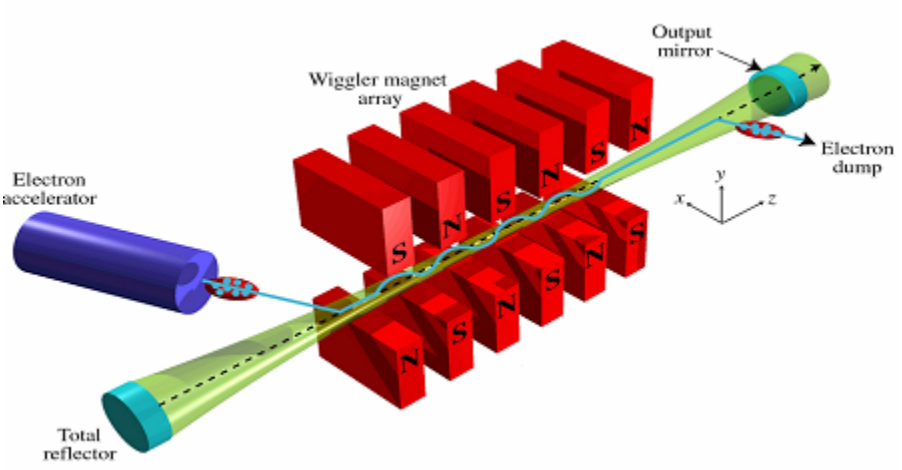

Figure 6. Undulator. Inside the undulator, an alternating magnetic field causes the relativistic electron beam to "wiggle", which causes the electrons to emit radiation. This schematic does not depict the number of undulator periods proposed for the MW class FEL, it merely depicts general undulator design.

The electrons that were generated within the photoinjector and accelerated by the linear accelerator to relativistic energies are passed through the undulator, which contains a static, periodic magnetic field over a number of periods. This magnetic field causes the electrons to "wiggle" which in turn, causes the electrons to emit radiation due to their acceleration in the transverse direction. This radiation is trapped within the optical resonator cavity between two mirrors, which straddle the undulator. This light is amplified by follow-on electron pulses, which undergo stimulated emission. The dimensions of the undulator and the optical cavity are such that the radiation produced from each electron pulse is coherently added to the energy already in the cavity. The

electrons leaving the undulator have given up a certain percentage of their energy to the optical beam and are now 180 degrees out of phase with the alternating RF fields in the LINAC.

The undulator design for the MW class weaponized FEL consists of the following parameters:

Undulator Design Parameters	
Undulator Length	L=43cm
Number of Undulator Periods	N=16
Undulator Wavelength	$\lambda_o = 2.7\,\text{cm}$
Undulator Field Strength	B_u=0.8T
Extraction	$\eta = 3.8\%$
Resonator Cavity Length	S=16m
Optical Beam Waist Radius	$w_o = 0.12\,\text{mm}$
Optical Mirror Spot Size Radius	$w(z) = 2.5\,\text{cm}$
Power out	P_{out}=1.8MW

Table 1 Undulator Design Parameters.

These parameters are based on a 110 MeV electron beam delivered to the undulator from the LINAC[Campbell, pp25].

5. Beam Dump

The electron beam leaves the undulator with 3.8% less energy (extraction efficiency) and a 14% energy spread induced by the FEL interaction. This de-energized electron beam reenters the beam pipe and is transported back to the LINAC where most of the electron beam energy is recycled back to the LINAC to help accelerate newly generated electrons from the photoinjector. The remainder of the electron beam is steered toward the beam dump for disposal.

The beam dump consists of various electrophylic materials such as copper, graphite, and aluminum to reduce scattering of electrons, dissipate heat, and control radiation. Fresh water cooling supplied by the auxiliary system is required to remove heat.

6. Beam Energy

It may be helpful in describing the electron beam system to follow the energy and power of the beam as it passes from component to component. This makes it easy to discuss energy generation, recovery and efficiency.

Initially, the photoinjector will produce a 7 MeV electron beam with 4.2 MW of power. This beam is transported to the LINAC where it is accelerated to 110 MeV and 66 MW of power. Once the beam gets to the undulator, a certain percentage of the beam's energy is used in the creation of the laser light. In this case, the single pass extraction efficiency of the undulator is 3.8%, which means 4.2 MeV and/or 2.5 MW of power are extracted from the electron beam for the generation of the optical beam. The electron beam then exits the undulator with approximately 105.8 MeV of energy, 63.5 MW of power, as it travels back to the LINAC for energy recovery. As mentioned before, the LINAC is receiving a 7 MeV, 4.2 MW, beam from the photoinjector, and now it is also receiving a 105.8 MeV beam from the undulator. The total input electron energy to the LINAC is approximately 112.8 MeV or 67.7 MW of power. Since the LINAC only requires an E_{acc} of 110 MeV, or 66 MW, the remaining 2.8 MeV, or 1.7 MW of power are diverted to the electron beam dump for disposal.

B. OPTICAL BEAM GENERATION AND CONTROL SYSTEM

The next major system is the optical beam generation and control system which is responsible for the creation, transport and pointing of the actual laser beam. As mentioned before, the laser beam is created within the undulator by the emission from laterally accelerated ("wiggled") electrons. The laser light is stored between the mirrors of the resonator cavity as it is amplified by follow-on electron beam pulses. On a continuous basis, a certain percentage of the beam exits the resonator cavity and enters the optical beam pipe (not the electron beam pipe) where it is transported to the director to be pointed and fired at the intended target.

1. Undulator

The undulator is considered an exchange component between the electron beam and the optical beam. Section II.A.4 focused on the electron beam aspect of the undulator. Here, the focus will be on the creation of the laser beam itself.

The generation of radiation by the "wiggling" of electrons does not alone constitute a laser. That radiation must be amplified considerably in order to produce the output power necessary to successfully conduct an engagement. The amplification process occurs within the undulator as "wiggled" electrons add radiation to the radiation already stored in the resonator cavity from previous electron beam pulses. The radiation field of the stored light leads to stimulated emission from the electrons which creates coherent laser radiation over a number of passes. The term "pass" or "passes" is used to describe the amplification process of one electron beam pulse as it "passes" through the undulator and interacts with a single pulse of light.

During the journey down the undulator, some electrons will gain energy while others lose energy. This gain and loss of energy will cause the electrons to "bunch" within each optical wavelength, leading to coherent radiation and "laser" light. The fraction of the total electron beam energy lost per pass is called the *extraction*.

2. Resonator Cavity

The purpose of the resonator cavity is to store emitted radiation between the two resonator mirrors to assist in the amplification process. The separation distance between the mirrors is crucial in the amplification of pulses and must be adjusted to ensure synchronization between the electrons and light. This condition is called resonance and will be discussed further in Chapter III, FEL Theory.

In order for the laser to escape the resonator cavity for use, one of the mirrors must be partially transmissive. This means that a certain percentage of laser light is allowed to pass through the mirror into the optical beam pipe and subsequently to the beam director. The amount of light that is transmitted through the mirror must equal the amount of light generated by the electron beam interaction in order to preserve a steady-state saturation level. Light can also be passed to the optical beam pipe by using a smaller radius mirror on one side of the resonator cavity instead of a transmissive mirror.

In this case the light passes around the mirror, rather than through it, allowing the proper percentage of light to escape the cavity.

3. Optical Beam Pipe

After passing through the transmissive mirror of the resonator cavity, the optical beam enters the optical beam pipe for transport. The purpose of the optical beam pipe is to transport the optical beam from the undulator to the beam director. The pipe may branch off at specific locations in order to feed more than one director from a single laser source. Much like in the electron beam pipe, the optical beam will travel down the longitudinal axis of the pipe, and be transported toward the director by a series of mirrors and lenses.

4. Beam Director

Located on the exterior of the ship, the beam director is the final component of the optical beam generation and control system. Mounted on a rotating base and fitted with a azimuthally elevating optical mirror assembly, Figure 7, the laser can conceivably engage targets over a hemispherical volume centered at the ship. The only limitation would be range and ship cut-outs (which can be reduced if more than one director is installed on the platform).

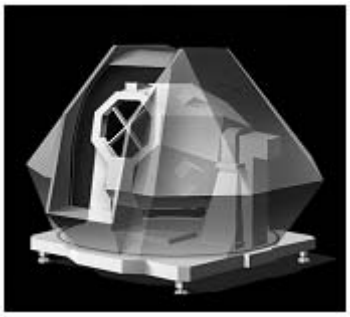

Figure 7. Conceptual design of an FEL director assembly.

One of the most critical components of the beam director will be the optics system. Environmental conditions at sea which can drastically affect the performance of the laser beam as it propagates through the atmosphere. Atmospheric turbulence, thermal blooming, scattering and other environmental effects can warp the beam and distort the phase front, dispersing the laser's power and reducing the overall probability of kill. One way to mitigate some affects of the atmosphere is through adaptive optics, which work

to purposely distort the optical beam wave front in a manner inverse to the expected atmospheric distortion. In consequence, as the beam propagates through the atmosphere, it actually reconstructs the proper wave front at the point of engagement. This allows for greater range and power on target through non-uniform atmospheric conditions.

C. AUXILIARY SYSTEM

Although not directly involved in the generation of light, auxiliary systems are responsible for supplying power, cooling, vibration control and the shielding necessary to maintain a stable and efficient FEL.

1. Power

The two primary means by which sufficient power can be generated for a megawatt class FEL are energy storage and direct power generation.

Since existing shipborne electric generators do not supply sufficient power to support megawatt class FEL operations, energy storage devices would be necessary to place FEL's on current platforms. Flywheels and capacitor banks could store energy from the ship's service power distribution system to provide the laser with immediate power at sufficient levels for a limited number of engagements. Once the storage devices are drained of their energy, they must be recharged before additional engagements can be made. While energy storage devices are a possible near term solution, they present numerous issues concerning weight distribution, damage control procedures, tactical considerations, and space requirements.

Many of the problems associated with energy storage devices will be solved through direct power generation. The Navy's next generation surface combatant (DDX) will be designed around the Integrated Power System (IPS) consisting of a 160 MW electric generator capable of supplying the requisite power for near continuous FEL utilization.

2. Cooling

The megawatt class FEL generates considerable heat. The three major components requiring heat dissipation are the beam dump, resonator mirrors and the RF superconducting structures. The beam dump alone must dissipate approximately 1.7 MW of power during FEL operation. While the dump is constructed of highly conductive

materials capable of rapidly dissipating heat, additional means of heat removal such as fresh water cooling are required to ensure that overheating and component failure do not occur. Fresh water cooling of the beam dump would be accomplished by passing fresh water cooling pipes through the beam dump allowing the heat to be removed from the dump through basic heat transfer, Figure 8. Similar fresh water heat transfer systems are installed in ships throughout the fleet and are capable of dissipating heat far greater than 1.7 MW.

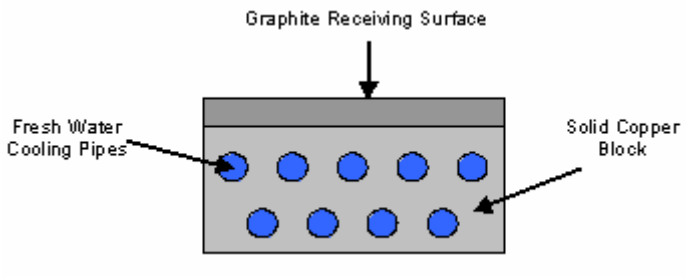

Figure 8. Cross-section of a fresh water cooled beam dump.

The RF superconducting structures associated with the photoinjector and linear accelerator represent the greatest source of heat within the FEL. Heat is generated within these structures by high voltage electric fields; their temperature must be maintained within 1ºC or better by a liquid helium refrigeration unit in order to enhance system efficiency and minimize component thermal expansion.

3. Vibration Control

Precisely aligned components within the FEL are sensitive to vibrations caused by ship flexing and external system interfaces. These vibrations can cause system degradation, failure, and personnel injury if unaccounted for. To mitigate the effects of vibration, critical systems components are shock mounted to reduce vibration between components. Additionally, within the optical resonator cavity, an active laser alignment system will keep the mirrors within operational limits.

4. Shielding

Electromagnetic radiation from accelerating electrons represents a serious shipboard hazard to sailors charged with operating and maintaining the FEL and the delicate electronic equipment necessary to operate it. Shielding requirements sufficient

to protect personnel yet small/light enough to satisfy space/weight restrictions on board ships are still being researched. One of the major sources of radiation for an FEL is the beam dump. Fortunately, the recirculation FEL design described in this chapter discharges only low energy electron pulses into the beam dump, therefore significantly reducing the required radiation shielding.

THIS PAGE INTENTIONALLY LEFT BLANK

III. FREE ELECTRON LASER THEORY

Now that a detailed description of a Free Electron Laser has been established, a more intensive mathematical discussion is warranted. Early descriptions of FEL theory utilized quantum electrodynamics[Madey], but the development of a classical approach[Colson] has proven to be accurate and easier to understand.

A. RESONANCE

In order for an FEL to achieve gain, a transfer of energy from the electron beam to the optical mode must occur. The optimum energy exchange occurs when one wavelength of light passes over a single electron in one undulator period. This situation is called the "resonance condition" and can be most easily described as a photon/electron "race." In this analogy, the photon and the electron race over one undulator period, the photon winning by one optical wavelength. As the electron oscillates through one undulator period, λ_o, it emits one wavelength of light. Figure 9 shows a diagram of the photon/electron race.

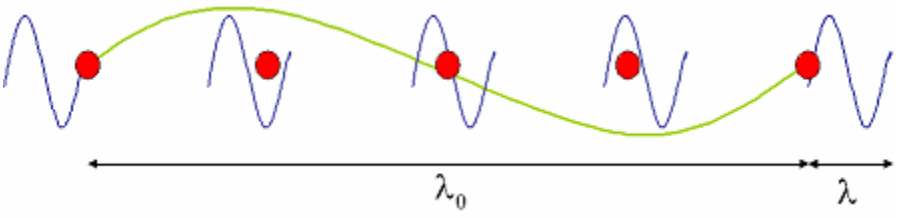

Figure 9. Photon-Electron Race

The optical wavelength (photon) λ is shown in blue, the electron is red, and the undulator wavelength λ_o is green. The undulator-optical wavelength relationship, or resonance condition, can be developed from the race. The time it takes an electron to travel through one undulator wavelength λ_o at speed v_z, is equivalent to the time it takes for the photon to travel a distance $\lambda_o + \lambda$ at the speed of light so that

$$\frac{\lambda_o}{v_z} = \frac{\lambda_o + \lambda}{c}. \tag{3.1}$$

Rearranging so as to solve for λ, with $\beta_z = v_z / c$,

$$\lambda = \left(\frac{1-\beta_z}{\beta_z} \right) \lambda_o \,. \tag{3.2}$$

This is the resonance condition and relates λ, λ_o, and β_z.
Now taking a look at the Lorentz factor,

$$\gamma = \frac{1}{\sqrt{1-\beta_z^2-\beta_\perp^2}}\,, \tag{3.3}$$

where $\beta_\perp = K/\gamma$ is the transverse component of the dimensionless electron velocity and $K = eB_u\lambda_o/(2\pi c^2 m_e)$ is the undulator parameter as will be shown later. Solving for β_z with $\gamma \gg 1$ yields

$$\beta_z = \sqrt{1-\frac{1+K^2}{\gamma}} \approx 1-\frac{1+K^2}{2\gamma^2}\,. \tag{3.4}$$

Inserting equation (3.4) into equation (3.2) provides a new expression for the optical wavelength in terms of γ

$$\lambda = \frac{\left[1-\left(1-\frac{1+K^2}{2\gamma^2}\right)\right]}{\left(1-\frac{1+K^2}{2\gamma^2}\right)}\lambda_o\,. \tag{3.5}$$

Since K is of order unity and $\gamma >> 1$, then $(1+K^2)/2\gamma^2 << 1$, so that the resonance condition becomes

$$\lambda \approx \left(\frac{1+K^2}{2\gamma^2}\right)\lambda_o \approx \frac{\lambda_o}{\gamma^2}\,, \tag{3.6}$$

to the first order in γ^{-2}, and with $K \approx 1$, for typical FEL parameters.

This form of the resonance condition demonstrates that for a given undulator, the wavelength of light can be modified by changing the electron energy and the undulator magnetic field B_u through K.

The transverse electron motion is induced by the undulator, resulting in radiation in the longitudinal direction. The combination of the magnetic field of the undulator and

the optical wave produces a pondermotive wave. This wave travels slower than the optical wave and can produce an exchange of energy if in resonance with the electrons. The pondermotive wave causes some electrons to speed up and others to slow down leading to electron bunching. This bunching is crucial since stimulated emission occurs when the electrons form coherent bunches within each optical wavelength. [Colson]

B. ELECTRON MOTION

1. Pendulum Equation

The microscopic motion of the electron can be described through the pendulum equation. As mentioned previously, relativistic electrons are injected down the longitudinal axis of the helical undulator (z-axis) and interact with the undulator's magnetic field and circularly polarized optical plane wave,

$$\vec{B}_u = B(\cos k_o z, \sin k_o z, 0),$$
$$\vec{B}_s = E(\sin\psi, \cos\psi, 0),$$
$$\vec{E}_s = E(\cos\psi, -\sin\psi, 0),$$

where B is the undulator magnetic field amplitude, $k_o = 2\pi/\lambda_o$ is the undulator wave number, E is the electric and magnetic field amplitude of the optical wave (in cgs units) and $\psi = kz - \omega t + \phi$ is the optical wave phase, where $k = \omega/c$ is the optical wave number and ϕ is the initial optical phase at $t=z=0$.

Since the electron beam energy is so large, the coulomb forces between the individual electrons can be ignored, therefore the total force acting on the electrons can be defined by the Lorentz force equation, [Griffiths].

$$\frac{d(\gamma\vec{\beta})}{dt} = -\frac{e}{m_e c}\left[\vec{E}_s + \vec{\beta}\times(\vec{B}_s + \vec{B}_u)\right] \tag{3.7}$$

Substituting the electric and magnetic fields listed above into equation (3.7), equations for the transverse component of the dimensionless electron velocity can be determined. Following the substitutions, the x-component of equation (3.7) can be written as

$$\frac{d(\gamma\beta_x)}{dt} = -\frac{e}{m_e c}\left[E(1-\beta_z)\cos\psi - B\beta_z \sin k_o z\right].$$

Since the electrons are relativistic, $\beta_z \approx 1$, therefore the first term within the brackets goes to zero leaving the simplified x-component term,

$$\frac{d(\gamma\beta_x)}{dt} = \frac{eB\beta_z}{m_e c}\sin k_o z \tag{3.8}$$

The same process can be followed to determine the y-component, leading to

$$\frac{d(\gamma\beta_y)}{dt} = -\frac{eB\beta_z}{m_e c}\cos k_o z \tag{3.9}$$

Equations (3.8) and (3.9) can be combined to yield

$$\frac{d(\gamma\vec{\beta}_\perp)}{dt} \approx -\frac{eB\beta_z}{m_e c}(-\sin k_o z, \cos k_o z, 0) \tag{3.10}$$

which by integrating yields

$$\gamma\vec{\beta}_\perp = \frac{-eB}{mc^2 k_o}(\cos k_o z, \sin k_o z, 0)\,. \tag{3.11}$$

Considering $K = eB\ /(c^2 m_e k_o)$, the magnitude of the transverse component of the dimensionless electron velocity, $\beta_\perp$, is,

$$\beta_\perp = \frac{K}{\gamma}$$

In the presence of light, the rate of change of the electron energy is $(d/dt)\gamma mc^2 = \vec{F}\bullet\vec{v}$, for example:

$$\frac{d\gamma}{dt} = \dot{\gamma} = -\frac{e}{m_e c}\vec{\beta}\bullet E_s = -\frac{e}{m_e c}E(\beta_x\cos\psi - \beta_y\sin\psi)$$

By the definition of *K,* equation (3.11), and the trigonometric identity $\cos A\cos B - \sin A\sin B = \cos(A+B)$,

$$\dot{\gamma} = \frac{eKE}{m_e c\gamma}\cos(k_o z + \psi) = \frac{eKE}{m_e c\gamma}(\zeta + \phi) \tag{3.12}$$

where $\zeta = (k + k_o)z - \omega t$ is defined as the electron phase with respect to the pondermotive wave. Differentiating this electron phase twice, a relationship for the time derivative of the fractional electron velocity in the longitudinal direction is obtained,

$$\dot{\zeta} = (k + k_o)\dot{z} - \omega = (k + k_o)\beta_z c - \omega$$

$$\ddot{\zeta} = (k + k_o)\dot{\beta}_z c \tag{3.13}$$

therefore

$$\dot{\beta}_z = \frac{\ddot{\zeta}}{(k + k_o)c}. \tag{3.14}$$

Rearranging equation (3.3) yields,

$$\frac{\left(1 + K^2\right)}{\gamma^2} = 1 - \beta_z^2.$$

Taking the time derivative of both sides of this equation gives,

$$\frac{\dot{\gamma}}{\gamma} = \frac{\gamma^2 \beta_z \dot{\beta}_z}{(1 + K^2)}. \tag{3.15}$$

Inserting equation (3.14) into equation (3.15) we find,

$$\frac{\dot{\gamma}}{\gamma} = \frac{\gamma^2 \beta_z \ddot{\zeta}}{(1 + K^2)(k + k_o)c} \tag{3.16}$$

Since the electrons are relativistic, $\beta_z \approx 1$ and $k >> k_o$, equation (3.15) becomes,

$$\frac{\dot{\gamma}}{\gamma} \approx \frac{\gamma^2 \ddot{\zeta}}{(1 + K^2)kc} = \frac{\lambda \gamma^2 \ddot{\zeta}}{(1 + K^2)2\pi c}. \tag{3.17}$$

Further simplification can be accomplished by substituting in the resonance condition, equation (3.6), and setting $K \approx 1$,

$$\frac{\dot{\gamma}}{\gamma} = \frac{\lambda_o \ddot{\zeta}}{4\pi c}. \tag{3.18}$$

Combining this equation with equation (3.12) and solving for the second derivative of the electron phase we are left with,

$$\ddot{\zeta} = \frac{2\omega_o eKE}{m_e c\gamma^2} \cos(\zeta + \phi). \tag{3.19}$$

Equation (3.19) is a form of the simple pendulum equation and describes the electrons dynamics.[Colson] In this form, the cosine term defines whether each electron gains or surrenders energy to the optical mode. The electrons with a phase between $-\pi/2$ and $\pi/2$ gain energy from the optical field and therefore accelerate. Electrons with a phase

between $\pi/2$ and $3\pi/2$ lose energy to the optical field and therefore decelerate. The resulting bunching of the electrons leads to stimulated emission.

C. OPTICAL WAVE EQUATION

While the pendulum equation described how the motion of the electrons is affected by the presence of an optical mode, this section on the Optical Wave Equation will demonstrate how the optical mode is affected by the electron beam. The Maxwell wave equation[Jackson] that governs the propagation of the optical mode is given by

$$\left(\nabla^2 - \frac{1}{c^2}\frac{\partial^2}{\partial t^2}\right)\vec{A} = -\frac{4\pi}{c}\vec{J}_\perp \tag{3.20}$$

where $\vec{J}_\perp$ is the transverse current density and $\vec{A}$ is the vector potential, related to the circularly polarized plane optical wave previously mentioned,

$$\vec{B}_s = \vec{\nabla} \times \vec{A}\,. \tag{3.21}$$

writing $\vec{A}$ in terms of z and t leads to the form,

$$\vec{A}(z,t) = \frac{E(z,t)}{k}(\sin\psi, \cos\psi, 0)\,. \tag{3.22}$$

Assuming that the amplitude and the phase of the optical mode vary slowly in both time and space over an optical wavelength, then

$$\frac{\partial E}{\partial t} \ll \omega E, \frac{\partial \phi}{\partial t} \ll \omega\phi,$$
$$\frac{\partial E}{\partial z} \ll kE, \frac{\partial \phi}{\partial z} \ll k\phi,$$

and it is therefore possible to show that the governing wave equation (3.20) can be simplified to

$$\begin{aligned}\left(\frac{\partial E}{\partial z} + \frac{1}{c}\frac{\partial E}{\partial t}\right) &\approx -\frac{2\pi}{c}\vec{J}_\perp \cdot \hat{\varepsilon}_1 \\ \left(\frac{\partial \phi}{\partial z} + \frac{1}{c}\frac{\partial \phi}{\partial t}\right)E &\approx \frac{2\pi}{c}\vec{J}_\perp \cdot \hat{\varepsilon}_2\end{aligned} \tag{3.23}$$

where $\hat{\varepsilon}_1$ and $\hat{\varepsilon}_2$ are unit vectors,

$$\begin{aligned}\hat{\varepsilon}_1 &= (\cos\psi, -\sin\psi, 0)\\ \hat{\varepsilon}_2 &= (\sin\psi, \cos\psi, 0)\end{aligned}.$$

The transverse currents can then be defined as the sum of each electron charge having a transverse velocity $\beta_\perp c$,

$$\vec{J}_\perp = -ec\sum_i \vec{\beta}_\perp \delta^3(\vec{x}-\vec{r}_i) = ec\sum_i \frac{K}{\gamma}(\cos k_o z, \sin k_o z, 0)\delta^3(\vec{x}-\vec{r}_i)$$

where $\vec{r}_i$ is the position of the i-th electron and δ^3 is the three-dimensional Dirac delta function. If we consider a large number of undulator periods, then the summation can be replaced by the volume element electron density ρ multiplied by the average electron phase on that volume element.[Colson] Therefore the previous equation can be written as,

$$\begin{aligned}\vec{J}_\perp \cdot \hat{\varepsilon}_1 &= \frac{ecK\rho}{\gamma}\left\langle \cos(\psi + k_o z)\right\rangle\\ \vec{J}_\perp \cdot \hat{\varepsilon}_2 &= \frac{ecK\rho}{\gamma}\left\langle \sin(\psi + k_o z)\right\rangle\end{aligned}. \tag{3.24}$$

Combining equations (3.23) and (3.24) and using $\zeta + \phi = \psi + k_o z$ gives the complex form of the optical wave equation

$$\left(\frac{\partial}{\partial z} + \frac{1}{c}\frac{\partial}{\partial t}\right)Ee^{i\phi} = -\frac{2\pi eK\rho}{\gamma}\left\langle e^{-i\zeta}\right\rangle. \tag{3.25}$$

When dealing with a long electron pulse, the spatial dependence in the longitudinal direction is no longer a concern which allows us to simplify the optical wave equation to,

$$\frac{1}{c}\frac{\partial}{\partial t}Ee^{i\phi} = -\frac{2\pi eK\rho}{\gamma}\left\langle e^{-i\zeta}\right\rangle.$$

This equation takes the form,

$$\frac{d(|a|e^{i\phi})}{d\tau} = -j\left\langle e^{-i\zeta}\right\rangle \tag{3.26}$$

where τ is the dimensionless time, the dimensionless optical field amplitude is $|a| = 4\pi NKLEe/\gamma^2 m_e c^2$, and $j = 8N(e\pi KL)^2 \rho/\gamma^3 m_e c^2$ is the dimensionless electron beam current. [Colson] This equation expresses the dependence of the rate of change in the optical field with the dimensionless current, *j,* and the average electron phase, ζ. If there is no current or no electron bunching, then the optical mode amplitude will not change.

D. GAIN

Gain, *G*, is the fractional power change in the optical field per pass through the undulator,

$$G = \frac{a_1^2 - a_o^2}{a_o^2}$$

where a_o and a_1 are the optical field strength at the beginning and end of the undulator, $\tau = 0$ and $\tau = 1$ respectively. In order to achieve gain, the electron beam must lose energy to the optical mode. Therefore one method of analyzing gain is to determine the change in the energy of the electrons. An electron's phase velocity is defined as follows,

$$\nu = \frac{d\zeta}{d\tau} = L[(k + k_o)\beta_z - k]. \tag{3.27}$$

Since $k_o << k$, a change in the electron phase velocity can be written as

$$\Delta\nu = Lk\Delta\beta_z . \tag{3.28}$$

Since $k = 2\pi/\lambda$, the resonance condition defined in equation (3.6) can be substituted into equation (3.28) to yield the relation

$$\Delta\nu = 2\pi N\left(\frac{2\gamma^2}{1+K^2}\right)\Delta\beta_z . \tag{3.29}$$

Using $\Delta\beta_z = \dot{\beta}_z \Delta t$ and $\Delta\gamma = \dot{\gamma}\Delta t$ so that equation (3.14) can be solved for $\Delta\beta_z$,

$$\Delta\beta_z = \frac{\Delta\gamma(1+K^2)}{\gamma^3\beta_z}$$

and substituted into equation (3.28) to get the relationship between $\Delta\nu$ and $\Delta\gamma$, assuming the approximation that $\beta_z \approx 1$,

$$\Delta\nu = 4\pi N \frac{\Delta\gamma}{\gamma} \tag{3.30}$$

This equation demonstrates that the change in the initial electron phase velocity is proportional to the fractional change in the electron energy.

Now, the number of electrons in a small volume of an optical wave, *dV,* is given by $N_e = \rho F dV$ where *F* is the filling factor and is defined as the cross-sectional area of the electron beam divided by the cross-sectional area of the optical beam. The average change of energy for an electron inside the undulator is

$$(\Delta\gamma) m_e c^2 \approx \frac{\gamma m_e c^2 \left(\langle\nu\rangle - \nu_o\right)}{4\pi N}$$

from equation (3.30) where $\langle\nu\rangle$ is the average post-undulator electron phase velocity for all electrons and ν_o is the initial electron phase velocity.

The average energy contained within the volume *dV* is given by

$$d\varepsilon_{o-beam} = \frac{E_s^2}{4\pi} dV$$

Therefore, gain in the optical field is

$$G = \frac{\Delta\varepsilon_{e-beam}}{d\varepsilon_{o-beam}} = -\frac{\rho F dV \gamma m_e c^2 (\langle\nu\rangle - \nu_o)/4\pi N}{2E_s^2 dV/8\pi} \tag{3.31}$$

$$G = \frac{\rho F \gamma m_e c^2 \left(\langle\nu\rangle - \nu_o\right)}{N E_s^2}$$

E. PHASE SPACE

A phase space plot is helpful in showing how a series of electrons evolve as they move through the undulator from $\tau = 0$ to $\tau = 1$. The y-axis plots the electron's phase velocity, ν, while the x-axis plots the electron's phase, ζ. The ζ axis represents a section of the electron beam that is approximately one optical wavelength long and is

traveling at the resonance velocity, $\nu = 0$. The plotted electrons move forwards or backwards based on their velocity relative to a resonant electron.

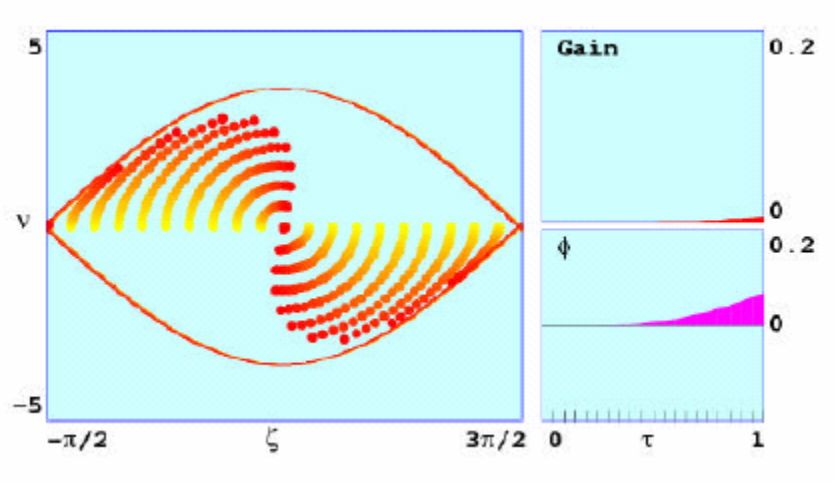

Figure 10. Phase Space Plot for $\nu_o = 0$

Figure 10 depicts the phase space evolution of 20 sample electrons as they pass through the undulator with an initial phase velocity $\nu_o = 0$. The color scale from yellow to red shows the change in the electron's position as it travels through the undulator. The electrons start off at the beginning of the undulator, equally distributed in phase with initial phase velocity $\nu_o = 0$ (yellow). At $\tau = 1$, the final positions of the electrons are indicated in red. In this figure, half of the electrons, from $-\pi/2$ to $\pi/2$, increase in phase velocity and gain energy from the optical field while the other half of the electrons, from $\pi/2$ to $3\pi/2$, decrease in phase velocity, hence losing energy to the optical field. The net energy exchange is 0 therefore there is no gain, *G,* as depicted in the upper-right hand portion of Figure 10. Despite insignificant gain, electron bunching does occur at approximately $\pi/2$, and the optical phase, ϕ, increases as shown in the lower-right hand plot.

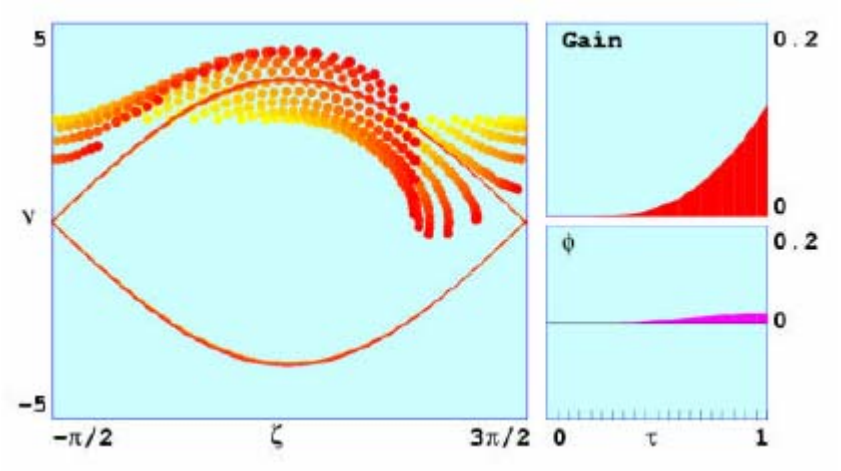

Figure 11. Phase Space Plot for $\nu_o = 2.6$

The phase space plot in Figure 11 portrays a condition where the initial phase velocity is above the resonance condition, at $\nu_o = 2.6$. In this example, a greater number of electrons have lowered in phase velocity as they evolve from $\tau = 0$ to $\tau = 1$, thus providing positive gain, $G \approx .12 = 12\%$, as evidenced by the upper-right hand plot of the figure.

THIS PAGE INTENTIONALLY LEFT BLANK

IV. SIMULATIONS OF HIGH-POWER FREE ELECTRON LASERS WITH STRONGLY FOCUSED ELECTRON AND OPTICAL BEAMS

A. INTRODUCTION

The immense power within the optical cavity, coupled with a small optical beam size required to produce a multi-megawatt class FEL, can cause severe resonator mirror damage. Mirror damage issues can be resolved by developing mirrors capable of withstanding greater intensity, lengthening the resonator cavity so as to increase the optical mode spot-size at the mirrors through diffraction, or by increasing the radius of curvature of the mirrors in order to induce a shorter Rayleigh length. A short Rayleigh length implies a narrow optical mode waist within the undulator, necessitating a strongly focused electron beam to improve electron beam/optical beam overlap. The short Rayleigh length option was studied utilizing three-dimensional computer simulations to determine the ramifications of off-axis shifting due to FEL component vibrations and to study the effects of strongly focused electron and optical beams on system performance.

1. Short Rayleigh Length

The Rayleigh length characterizes the growth of the optical beam caused by diffraction. From $z = 0$ to $z = z_o$ the optical mode doubles in area and for $z \gg z_o$, the growth in area is quadratic in z. Current design parameters utilize a Rayleigh length, $z_o \approx 1\,\text{m}$, resulting in an optical mode waist radius of $w_o = 0.56\,\text{mm}$ at the center of the resonator cavity, for a $\lambda = 1\,\mu\text{m}$ optical beam, using $w_o = \sqrt{z_o \lambda / \pi}$. To determine the optical spot size at the mirrors, $w(z)$, the following equation must be used

$$w^2(z) = w_o^2 \left[1 + \left(\frac{z}{z_o} \right)^2 \right]$$

where $z = S/2$ and S is the resonator length. Assuming $S = 16\,\text{m}$, the resulting optical spot size radius at the mirrors is 44.8 cm. If 25% of the stored light escapes through the transmissive mirror, then a 1 MW output power laser would require 4 MW of stored power within the resonator cavity. The intensity on the mirrors would therefore be

approximately 6.3 MW/cm^2, more than 30 times the damage limit of cooled sapphire mirrors with a transmissive coating. [Ref. 1]

Reducing the Rayleigh length to $z_o = 1.9$ cm increases the mirror spot size radius to 2.5 cm and decreases the overall mirror intensity to approximately 200 kW/cm^2. This intensity level is manageable utilizing current mirror technology. A short Rayleigh length implies a very narrow, intense optical beam at the undulator center where the electron beam and optical mode interact. If the electron beam radius is greater than the optical mode waist within the interaction region then those non-overlapping electrons will not contribute to the amplification of the stored light. So to achieve maximum efficiency within the undulator a narrow electron beam is necessary as well.

2. High Power FEL Parameters

Design parameters for MW class FEL's are constantly in flux as requirements and technology evolve. The parameters listed in this section describe a MW-class FEL. In order to utilize a shorter Rayleigh length of $z_o = 1.8$ cm the optical resonator cavity was simulated by the parameters listed in Table 2.

OPTICAL RESONATOR CAVITY PARAMETERS	
Optical Wavelength	$\lambda = 1\,\mu$m
Optical Cavity Length	$S = 12$ m
Power through Transmissive Mirror per Pass	28%
Optical Mode Waist Radius	$w_o = 0.1$ mm

Table 2 Optical Resonator Cavity Parameters for a MW-Class FEL (From [Ref. 2])

These parameters predict a mirror intensity of 210 kW/cm^2.

Since reducing the Rayleigh length causes the optical mode to rapidly expand, the interaction region is reduced necessitating a shorter undulator with fewer periods to avoid beam scraping against the edges of the undulator. Table 3 lists the undulator parameters used for the simulations.

UNDULATOR PARAMETERS	
Number of Periods	$N = 20$
Undulator Period	$\lambda_o = 3\,\text{cm}$
Undulator Length	$L = 60\,\text{cm}$
Undulator rms Parameter	$K = 2.8$

Table 3 Undulator parameters for MW-Class FEL (From [Ref. 2])

In order to produce an efficient, high quality optical beam utilizing the above listed parameters, the electron beam must be specifically defined, Table 4.

ELECTRON BEAM PARAMETERS	
Electron Beam Energy	$K_e = 185\,\text{MeV}$
Peak Current	$I_P = 3.2\,\text{kA}$
Average Current	$I_A = 0.8\,\text{A}$
Bunch Length	$l_e = 0.1\,\text{mm}$
Bunch Charge	$q = 1.1\,\text{nC}$
Pulse Repetition Frequency	$\Omega = 750\,\text{MHz}$
Average Power	$P_A = 148\,\text{MW}$
Required Extraction	$\eta \geq 0.7\%$
Beam Emittance (normalized)	$\varepsilon_n = 24\,\text{mm-mrad}$
Electron Beam Radius	$r_e = 0.14\,\text{mm}$

Table 4 Electron beam parameters for a MW-Class FEL (From [Ref. 2])

B. THREE DIMENSIONAL COMPUTER SIMULATIONS

Vibrations inherent to a maritime environment must be mitigated in order for a shipboard FEL to function properly. Considering an optical mode waist radius of only

0.1mm, even slight misalignment could cause reduced overlap between the electron beam and the optical field within the undulator, severely decreasing system performance.

A given accelerator has a fixed normalized beam emittance,

$$\varepsilon_n = \gamma r_e \theta_e$$

where γ is the Lorentz factor, r_e is the electron beam radius, and θ_e is the electron beam angular spread. For a typical FEL with an undulator on the order of a few meters in length, r_e and θ_e are arranged so that the electron beam does not grow significantly over the length of the undulator, hence optimizing the overlap between it and the optical mode. In order to achieve the same optimized overlap in a short Rayleigh length FEL, the electron beam must be strongly focused by the use of additional external focusing magnets. The resulting decreased r_e enhances both gain and efficiency while increasing the optical beam spot size on the resonator mirrors. [Ref. 2]

Considering the interaction region precision required for a short Rayleigh length FEL to function, a study of vibrational effects was conducted. One such vibrational condition was electron beam off-axis shift in the y-direction. Figure 12 depicts such a condition where the optical mode (blue) is confined within the bounds of the resonator cavity. The electron beam (red) is shown shifted in the y-direction a distance y_o from the undulator (green).

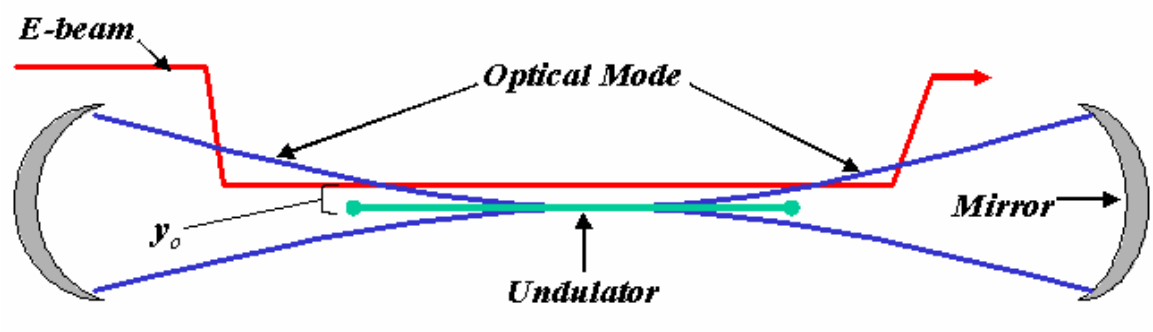

Figure 12. Electron Beam Off-axis Shift.

An additional area of study was the effect of a strongly focused electron and optical beam on the performance of an FEL with the previously listed parameters. Figure

13 portrays the focused electron beam (red) overlapping the optical mode (blue) within the undulator. The focused electron beam provides a reduced r_e and therefore an increased θ_e.

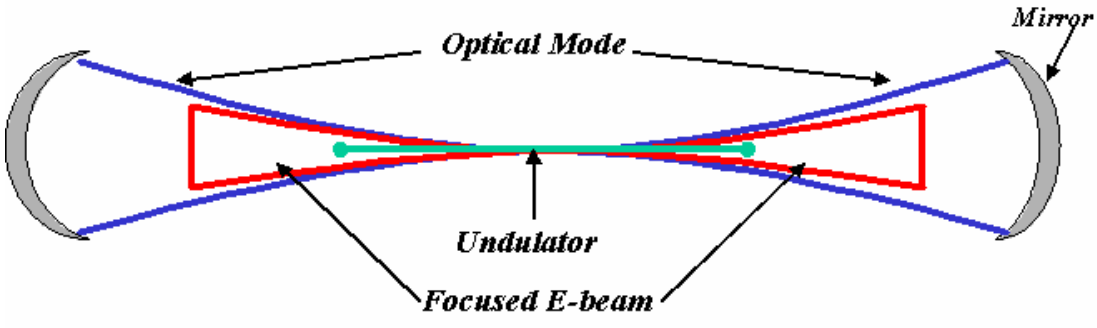

Figure 13. Strongly Focused Electron Beam.

1. Simulation Methods

The three dimensional (x, y, t) computer simulation used for this study included the effects of diffraction and optical mode distortion. The undulator is oriented along the z-axis, with the magnets normal to the y-axis and the static magnetic field along the x axis. For the simulation, all parameters were normalized; longitudinal lengths and time were normalized to the length of the undulator L, transverse lengths were normalized to $\sqrt{L\lambda/\pi}$ and angles normalized to $\sqrt{\lambda/L\pi}$.

In order to decrease runtime, simulations were initiated with a small amount of optical power. The electrons were given an initial spread in positions x, y and angles, θ_x, θ_y, determined by beam emittance and focusing. To study the effects of off-axis shift, a y_o value moves the beam off axis as shown in Figure 12. As the electrons pass through the undulator they undergo betatron motion oscillations in the yz-plane according to

$$y = (y_o + \Delta y)\cos\left(\omega_\beta\left(\tau - \tau_\beta\right)\right) + \frac{\theta_{yo} + \Delta\theta_y}{\omega_\beta}\sin\left(\omega_\beta\left(\tau - \tau_\beta\right)\right)$$

where the distance y_o is the beam shift off-axis, θ_{yo} is the off-axis tilt, Δy is a random shift due to the beam radial spread, $\Delta\theta_y$ is a random angle due to the beam angular spread and ω_β is the betatron frequency given by $2\pi NK/\gamma$. The time parameters, τ and

τ_β, are normalized to the length of the undulator. The electron position along the undulator axis is τ, while τ_β is the position of the electron beam focus. In studying the effects of off-axis shift, y_o was varied with $\theta_{yo} = 0.0$ and $\tau_\beta = 0.5$.

In the longitudinal direction, the electrons evolved in phase space according to the FEL pendulum equation described in Chapter III. An electron's phase velocity is given by

$$\nu = L\left[\left(k + k_o\right)\beta_z - k\right]$$

where k is the optical wave number given by $2\pi / \lambda$, k_o is the undulator wave number given by $2\pi / \lambda_o$, and $\beta_z = v_z / c$. If an electron is injected off-axis by a distance y_o, its phase velocity is modified by $\Delta\nu = -\left(\omega_\beta^2 y_o^2 + \theta_y^2\right)$. The optical wave front is started with an initial Gaussian profile and evolves over many passes until a steady state mode is obtained. The extraction is determined by

$$\eta = -\langle\Delta\nu\rangle / 4\pi N$$

where $\langle\Delta\nu\rangle$ is the shift in the average electron phase velocity due to the FEL interaction. [Ref. 2]

2. Simulation Output Format

Figure 14 is a sample output file from a three-dimensional simulation conducted to study the effects of an off-axis shift of the electron beam for a short Rayleigh length FEL with $z_o = 0.03$.

The upper right section of the output format displays the dimensionless parameters used for the run. In this example, the electron beam has a dimensionless current density of $j = 210$, and a dimensionless radius in the x and y directions of $\sigma_{x,y} = 0.3$. The electrons are injected into the N=20 period undulator with an initial phase velocity of $\nu_o = 7.33$. Both the electron beam and the optical mode are focused at

the center of the undulator, $\tau_\beta = \tau_W = 0.5$. The betatron frequency, $\omega_\beta = 0.7$ and the electron beam radius contribute to the determination of the dimensionless electron

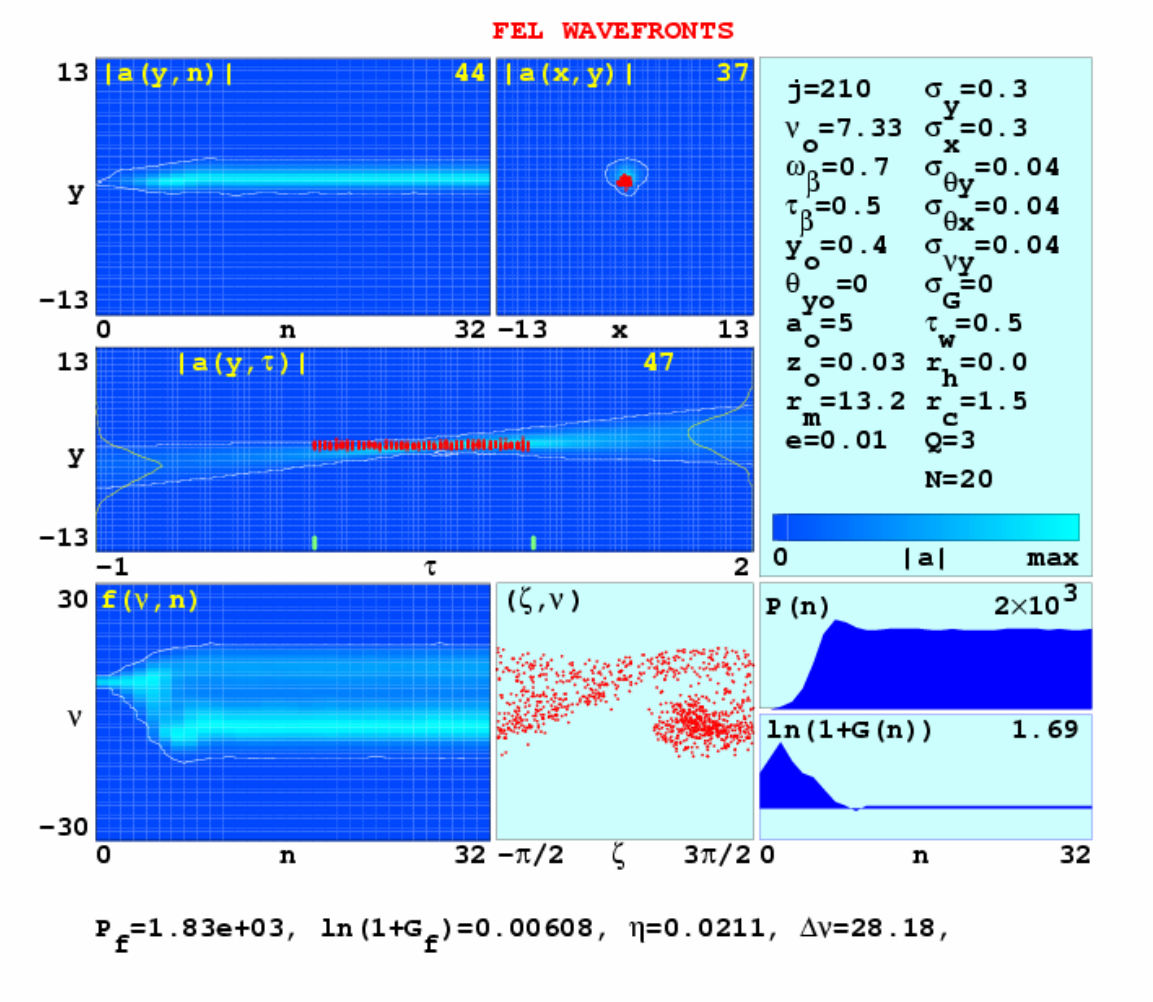

Figure 14. Three Dimensional Simulation Output Format

beam angular spread, $\sigma_{\theta x,y} = 0.04$. The dimensionless mirror radius, $r_m = 13.2$, and dimensionless radius of curvature, $r_c = 1.5$, determine the Rayleigh length, $z_o = 0.03$, and the edge loss per pass of 1%. The initial field strength of the run was $a_o = 5$. In this particular simulation the electron beam was shifted by $y_o = 0.4$ and there was no beam tilt, $\theta_{yo} = 0.0$.

The upper left and center plots of Figure 14 depict optical field intensity. The color scale for these plots is defined within the dimensionless parameters box, where light

blue indicates a maximum amplitude and dark blue indicates a zero amplitude region. The white contour line for all plots on this output format follow the 5% curve of the maximum optical field intensity at the cavity center. The upper left plot in particular shows a side view of the optical wavefront as it evolves over $n = 32$ passes. The upper center plot shows the optical wavefront head-on view at the end of the undulator over the same number of passes. The red dots indicate the position of sample electrons, showing the optical/electron beam overlap and final electron beam spread.

The middle center plot, $a(y,\tau)$, portrays a side view of the optical wavefront during the final pass through the cavity. Again, the electron/optical beam overlap region is evident by observing the sample electron positions (red dots) in reference to the maximum optical field intensity region (light blue). The yellow contour lines at the opposite ends of the plot represent the optical wave profile amplitude which corresponds to the power distribution on the resonator mirrors. In this simulation the mirror separation is 3 times the undulator length so it varies from $\tau = -1 \rightarrow 2$ while the undulator is from $\tau = 0 \rightarrow 1$, denoted by the yellow hash-marks at the base of the plot.

The lower-left plot describes the electron spectrum evolution. Electrons are injected with an initial phase velocity of $\nu_o = 7.33$. The electron energy spread increases in strong optical fields until it reaches a saturated state, in this case at approximately $n = 8$ passes. The plot to its immediate right represents the phase space position of the sample electrons during the final pass. This plot is useful in identifying electron bunching.

The final two plots in the lower-right-hand corner of the output file illustrate the power and gain evolution of the laser over the number of passes, *n*. Similar to the electron spectrum evolution plot, the optical field becomes saturated at approximately 8 passes, providing steady-state power. The final power, gain, extraction, and phase velocity spread are listed in a single line below the plots.

3. Simulation Results

a. Electron Beam Shift

In order to study the effects of electron beam shift on the performance of the FEL, multiple simulation runs were conducted varying the value of y_o from 0 to 1 at incremental steps of 0.1. This is a viable simulation method because shipboard vibrations

are on a kHz scale while electron and optical pulses are on a MHz scale. An experimental design tolerance for beam alignment of 0.01mm corresponds to a normalized value of $y_o = 0.023$. At each of these values of y_o the initial electron phase velocity, ν_o, was also varied in order to determine the peak extraction, η.

Figure 15 is a plot of steady-state extraction versus the initial phase velocity over three values of y_o. For each value of the electron beam shift, as the initial phase velocity

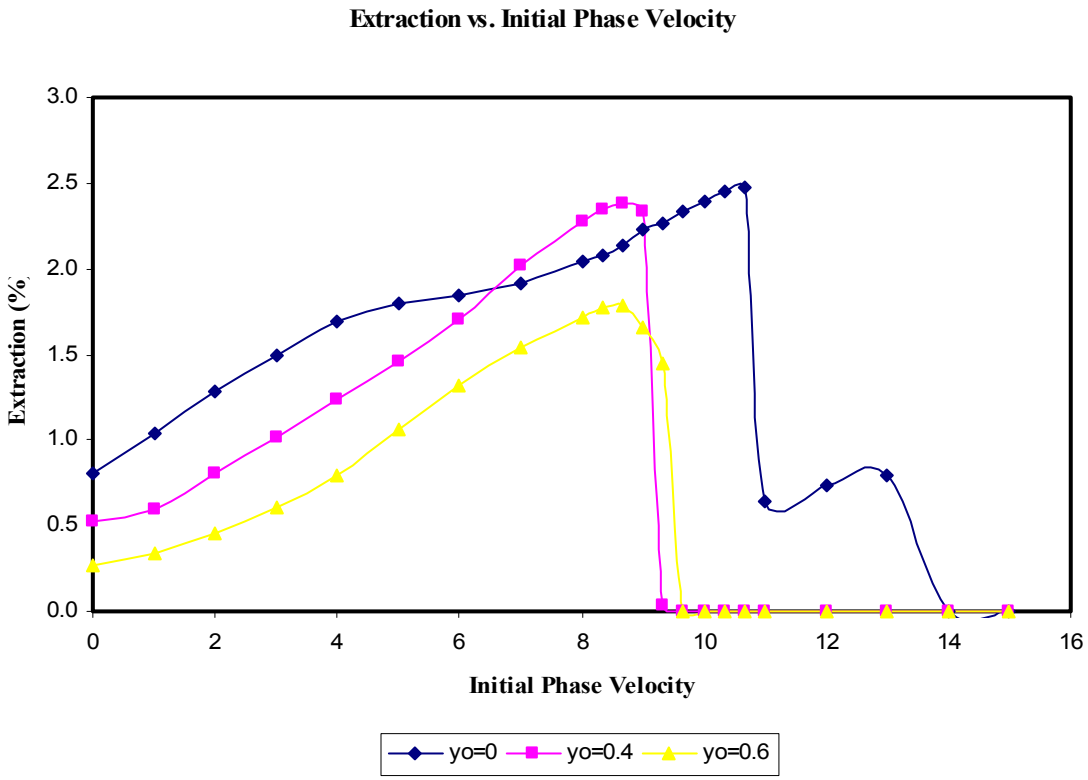

Figure 15. Single Pass Extraction Efficiency versus Initial Phase Velocity for Various Values of the Normalized Beam Shift.

increases from zero, so does the efficiency. Each peak corresponds to a value of ν_o where the FEL gain is just slightly above threshold. The highest peak extraction is approximately 2.5%, where there is no electron beam shift and the initial phase velocity is approximately $\nu_o = 10.66$. This is to be expected since at y_o=0, the optical mode and electron beam almost perfectly overlap. It can also be seen that extraction decreases as

the electron beam moves further off axis. Not only does extraction decrease, but the optimum initial phase velocity changes. Therefore, an electron beam shift can change the optical wavelength [Ref. 2] since a change in ν corresponds to $\Delta\nu = 2\pi N(\Delta\lambda/\lambda)$.

Referring back to Figure 14, the center-left plot suggests that the FEL interaction takes place close to the undulator center. If the electron beam is shifted off-axis, it is not aligned with the intense optical mode in the interaction region. This causes the entire optical mode to tilt. Regardless of the optical mode tilt, the optical power still reaches steady-state, but the extraction efficiency at y_o=0 is reduced from 2.5% to 2.1%.

All of the peak extraction values determined for each value of y_o were plotted to summarize the final results of the study. Figure 16 shows the peak extraction (at the optimum value of ν_o) versus the normalized electron beam shift y_o.

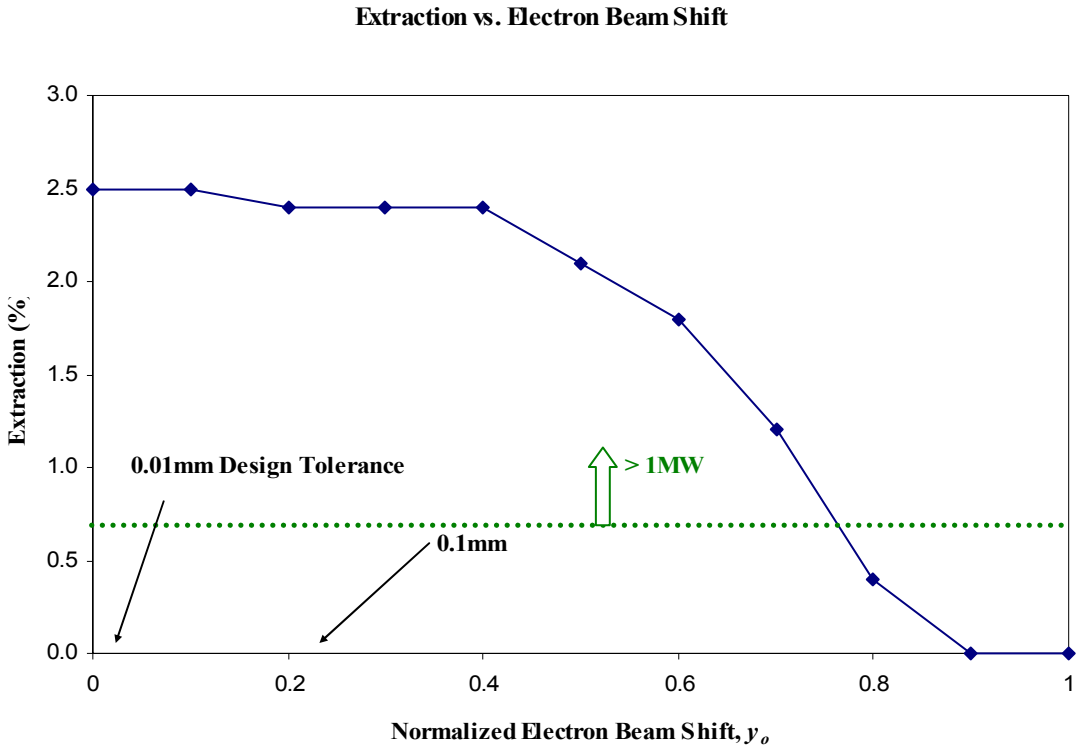

Figure 16. Peak Single-Pass Extraction versus the Normalized Electron Beam Shift

The normalized experimental design tolerance that corresponds to 0.01mm (y_o=0.023) is indicated by the arrow. Extraction values required to achieve 1MW power ($\eta = 0.7\%$) are those above the green dotted line. Here again the peak extraction steadily

deceases as the electron beam is shifted further off the optical axis, yet retains sufficient efficiency far beyond the experimental design tolerance to produce the required power. In fact the electron beam can be shifted nearly 3mm off-axis and still produce a 1 MW optical beam.

b. Electron Beam Focusing

When researching the effects of the electron beam off-axis shift, the normalized beam radius was maintained at a constant $\sigma_x = \sigma_y = \sigma_e = 0.3$ while y_o was varied. To study the effects of the strongly focused electron beam, y_o was held constant at 0 while the electron beam radius was modified from $\sigma_e = 0.3 \rightarrow 0.15$.

Decreasing the electron beam radius causes greater beam overlap in the interaction region hence increasing the single-pass extraction efficiency. This effect is presented in Figure 17 where peak extraction, η, is plotted against the normalized electron beam radius, σ_e. As the electron beam becomes more constricted, the peak

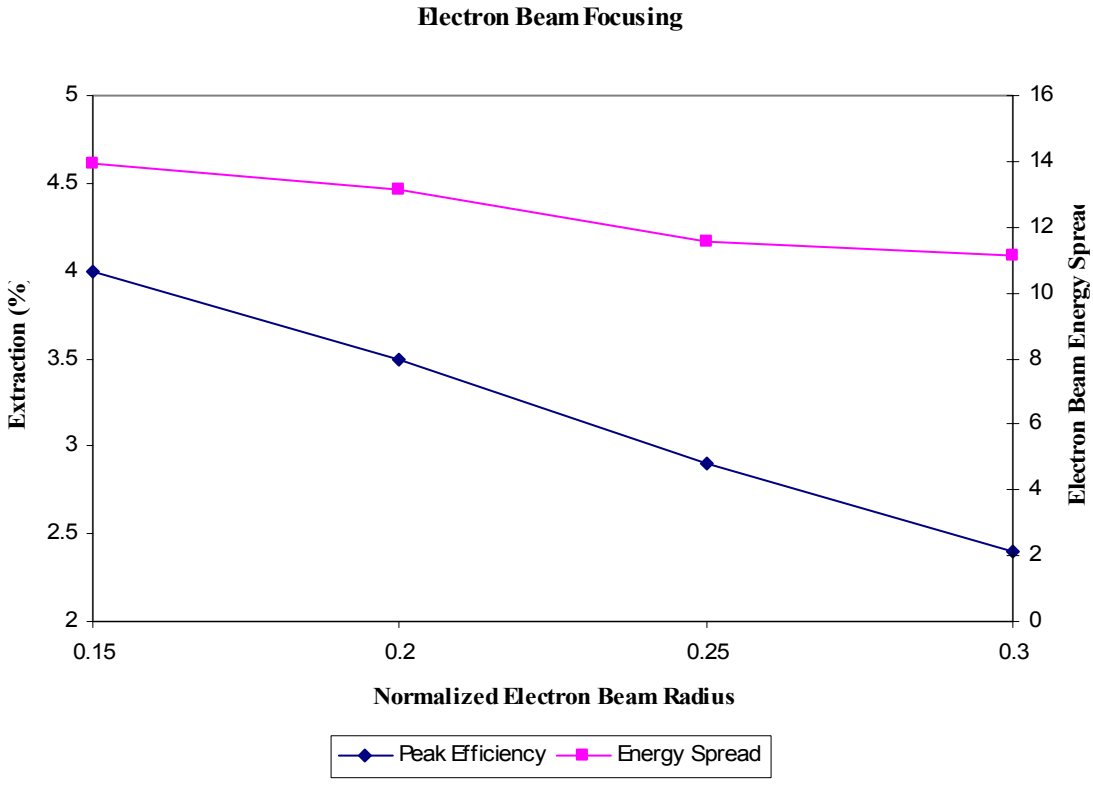

Peak Single-Pass Extraction and Induced Energy Spread versus Normalized Electron Beam Radius

extraction increases from roughly 2.4% to 4%, which in either case is greater than the requirement of 0.7%. This increase in extraction efficiency may allow for a reduced average current while still achieving the 1MW goal.

Figure 17 also plots the induced energy spread against the normalized electron beam radius against the induced energy spread of the beam. As with the peak extraction, the induced energy spread increases as the electron beam becomes more strongly focused, ranging from approximately 11% to 14%. The energy spread needs to be kept below the maximum allowable limit for safe electron recirculation of about 15%.

4. Conclusion

The proposed short Rayleigh length FEL provides a number of benefits to future shipboard designs. The short Rayleigh length induces a rapidly expanding optical mode, hence increasing the mirror spot size and decreasing optical mode intensity on the mirrors, reducing damaging effects. Since the short Rayleigh length necessitates a narrow optical mode waist within the interaction region, the possibility of reduced system performance due to vibrational offsets was studied. It was concluded though that even with electron beam off-axis shifts 30 times greater than the experimental design tolerances, sufficient extraction efficiency was achieved to lase at 1MW. Additionally, the more tightly the electron beam was focused in the interaction region the greater the peak extraction without the recirculation issues of a higher induced energy spread.

V. MULTIMODE SIMULATIONS OF A SHORT-RAYLEIGH LENGTH FEL

A. INTRODUCTION

While Chapter IV investigated short-Rayleigh length FEL tolerances to vibrational effects, specific design parameters are still required and warrant further research. A three-dimensional, multimode simulation program was used to study the effects of varying electron beam, undulator, and cavity parameters. For each set of parameters, the FEL is started in weak fields and allowed to evolve over many passes to steady-state. The single-pass peak extraction is then calculated [Ref. 3]. Extraction is defined as the amount of power that is transferred from the electron beam to the optical mode within the interaction region in the undulator.

Simulation methods and output format are nearly identical as those discussed in Chapter IV, and therefore explanations will not be repeated in this chapter.

1. High Power FEL Parameters

As mentioned previously, design concepts, systems requirements, and technology continue to evolve which has necessitated modification of high power FEL parameters. The parameters identified in this chapter describe the MW-class FEL design used specifically for this research and may be altered in the future. While these parameters may change over time, many research conclusions are not expected to vary significantly.

The resonator cavity simulation design yields an optical wavelength of $\lambda = 1\,\mu\text{m}$, and an optical cavity length of $S = 16\,\text{m}$. The optical mode waist radius, w_o, is determined by the normalized Rayleigh length as it changes from $z_o = 0.05 \rightarrow 0.12$ (normalized to the undulator length *L)*. While the undulator period is fixed at $\lambda_o = 2.7\,\text{cm}$, the undulator length *L* varies as the number of undulator periods *N* progresses through the range 8 to 20. The undulator parameter is K_{rms}=1.4. The electron beam is accelerated to energies of $K_e = 100\,\text{MeV}$ with peak and average currents of I_P=1.5kA and I_A =1.1A respectively. The electron bunch length of $l_b = 0.3\,\text{mm}$, charge $q = 1.5\,\text{nC}$, and pulse repetition frequency $\Omega = 750\,\text{MHz}$ all remain constant, while the

normalized electron beam waist radius takes on the values

$\sigma_e = \left(r_e / \sqrt{L\lambda / \pi} \right) = 0.06 \rightarrow 0.23$.

B. SIMULATION RESULTS

1. Variation of Undulator Periods

The first area of research focused on varying the length of the undulator by altering the number of undulator periods from $N = 8 \rightarrow 20$. The resonance parameter, ν_o , was varied independently to determine the optimum result for each value of *N*. The simulation results for extraction η as a function of the number of undulator periods are shown in Figure 18.

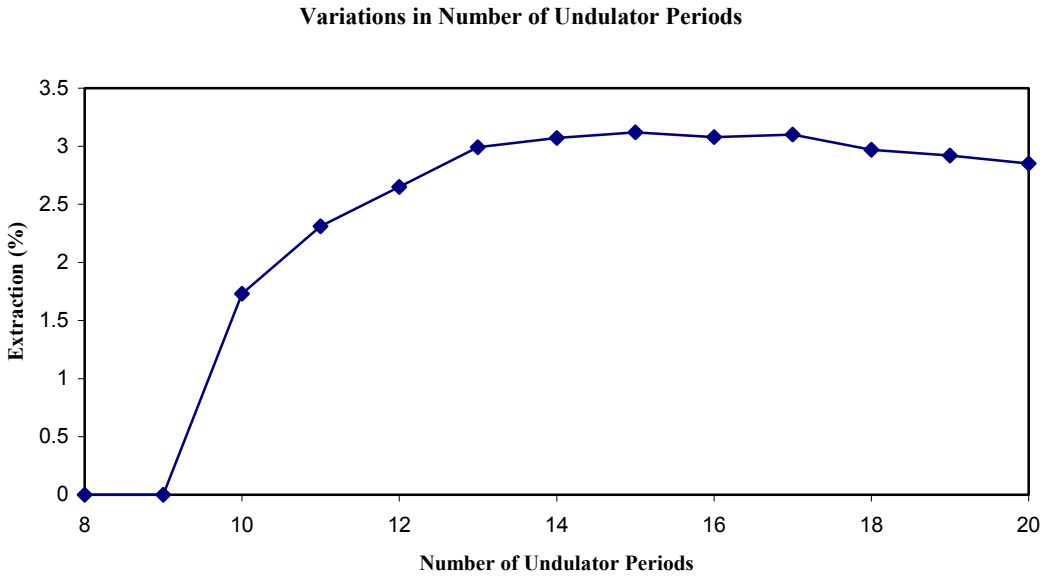

Figure 17. Simulation results for extraction, η, versus number of undulator periods *N*.

The results show that if there are too few undulator periods, *N*<10 in this case, the FEL is below threshold and therefore there is no extraction from the electron beam. Optimum extraction, $\eta \approx 3\%$, occurred when *N*=15 but slowly decreased as the number of undulator periods increased beyond *N*=15 due to lower optical saturation limit. Note that even though $z_o \approx \lambda_o$ and $z_o \ll L$ undulator periods away from the mode focus

definitively play a role in energy extraction. While the early periods do not contribute directly to energy extraction, they serve to "prepare" the electron beam by initiating the bunching process.

2. Variation of Electron Beam Waist Radius

To study the effects of varying the radius of the electron beam waist from $\sigma_e = 0.06 \rightarrow 0.23$, the transverse emittance, $\varepsilon_n = \gamma r_e \theta_e$, is held constant. The results of the simulations are illustrated in Figure 19 which shows that for a large beam radius, the extraction drops due to reduced overlap with the intense optical fields in the center of the undulator, whereas for a small beam radius the extraction drops due to the corresponding large angular spread of the electron beam[Ref. 3].

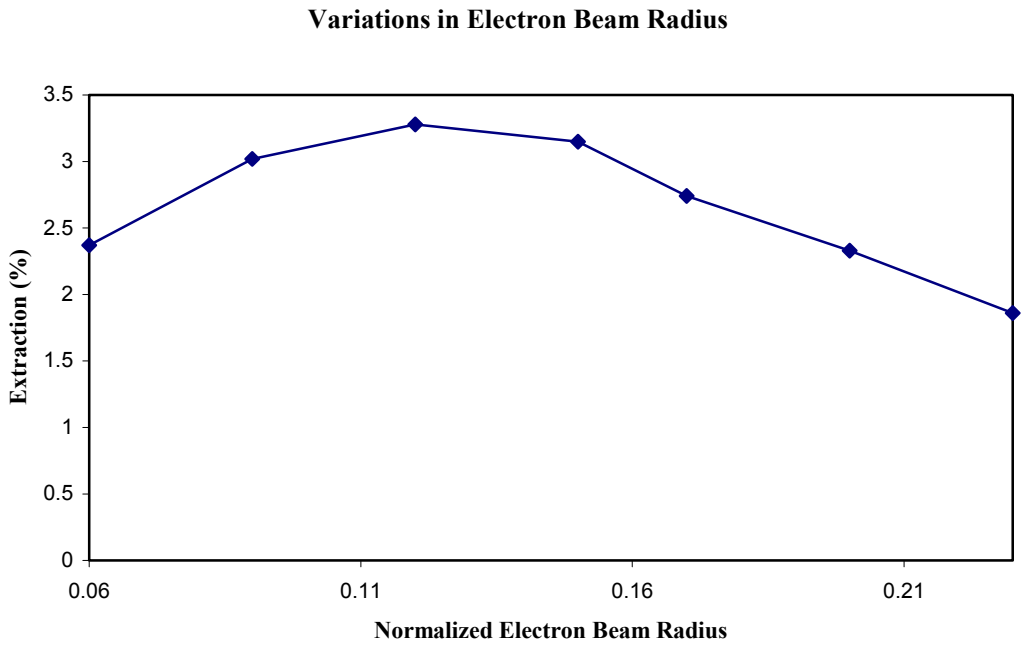

Figure 18. Simulation results for extraction, η, versus normalized electron beam radius, σ.

This effect can easily be identified by examining selected simulation output files. These files are identical in format to those described in Chapter IV. The $a(y,\tau)$ plot portrays a side view of the optical mode during the final pass through the undulator and shows the effects of varying the electron beam radius. Figure 20 is an example of a weakly focused beam where the electron beam waist is relatively large, $\sigma_e = 0.23$.

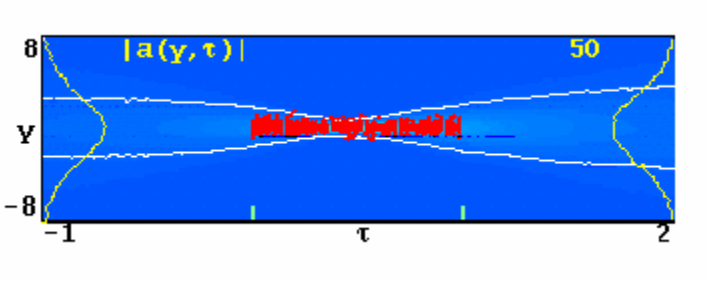

Figure 19. Simulation output file of a weakly-focused electron beam.

Here, the electrons (red) have a less than optimum overlap with the intense optical field (light blue) in the center of the undulator (undulator ends denoted by green tick marks).

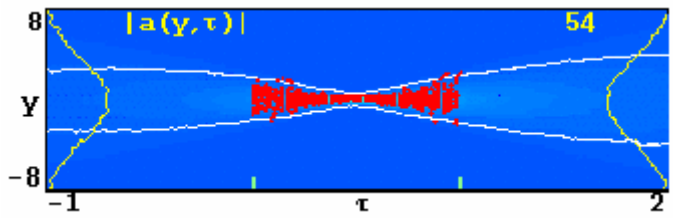

Figure 20. Simulation output of a strongly-focused electron beam.

Note that at the center of the undulator a number of electrons are near the outer edge of the optical mode indicated by the white contour lines at 5% of the peak optical intensity. The electron beam is too wide and reduces extraction. Conversely, a strongly focused electron beam, $\sigma_e = 0.06$, also results in a decreased extraction due to a large angular spread as seen in Figure 21. In this case, the electrons are near the outer edges of the optical mode at the end of the undulator. Between these two extremes there is an optimum electron beam radius. For these parameters, $\sigma_e = 0.12$ was the optimum normalized electron beam radius which provided an extraction of $\eta = 3.8\%$.

3. Variation of Normalized Rayleigh Length

Finally, simulations were conducted to study the effect of varying the Rayleigh length. As discussed in Chapter IV, the shorter the Rayleigh length, the faster the optical mode diffracts, leading to a reduction in mode spot size intensity on the mirrors. Figure 22 shows the simulation results of varying the normalized Rayleigh length from $z_o = 0.05 \rightarrow 0.12$.

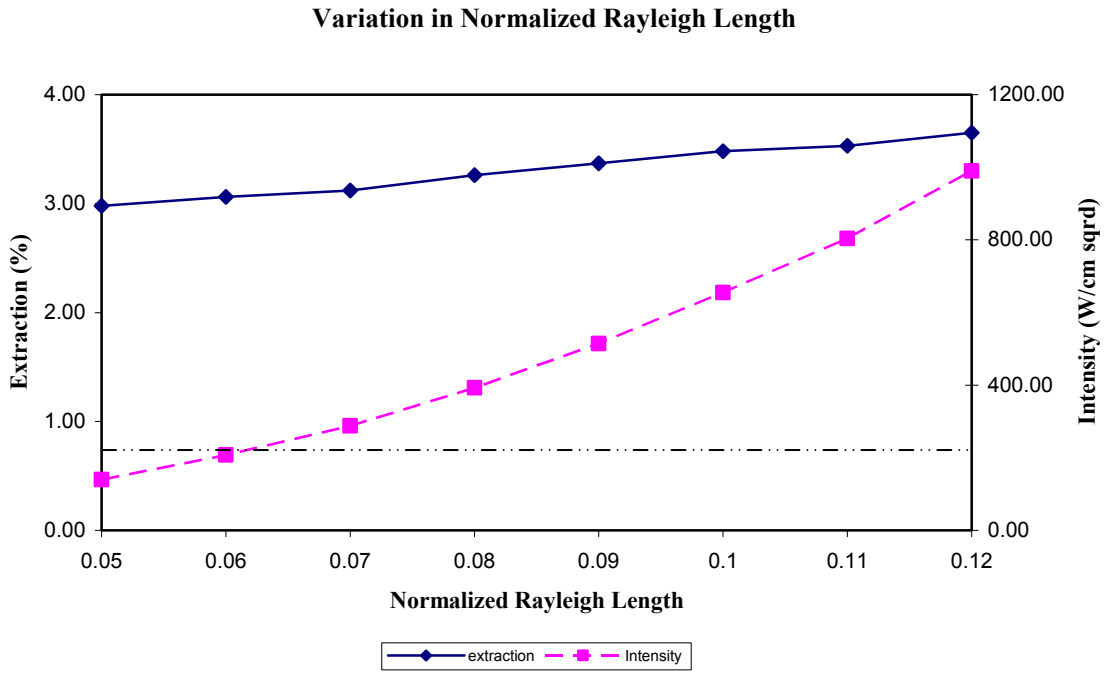

Figure 21. Simulation results for extraction, η, and mirror intensity versus normalized Rayleigh length, z_o.

As z_o is reduced the extraction (solid blue line) slowly drops, but the mirror intensity (dashed red line) is significantly reduced since the mode spot size at the mirror increases due to increased diffraction. Therefore to stay within the expected maximum mirror intensity limit of approximately I=200kW/cm^2 (horizontal grey dotted line), the Rayleigh length should be less than z_o=0.06.

C. CONCLUSION

The short-Rayleigh length FEL concept promises numerous benefits for a proposed shipboard system. Before the concept can become reality, specific design requirements must be identified, which motivated this research. While specific numerical values were determined, the greatest benefit to this research stems from the understanding of the relationships between FEL parameters. While specific values may change as parameters are scaled to meet MW-class requirements, the graph shapes and underlying concepts will probably remain the same, leading to a greater overall understanding of those relationships.

THIS PAGE INTENTIONALLY LEFT BLANK

VI. FEL CONCEPT OF OPERATIONS FOR NAVAL PLATFORMS

A. INTRODUCTION

The ultimate goal of FEL research at NPS is to develop a MW-class laser to be utilized as a point defense weapon system on naval at-sea platforms, from aircraft carriers to destroyers. A sound concept of operations (CONOPS) is crucial in the evolution of such a system to facilitate discussions concerning system usefulness, tactics, feasibility, cost effectiveness, and overall understanding. As a general guideline, a concept of operations establishes the baseline procedures for a system's usage and operation.

An FEL as a valid shipboard weapon system is still at least a decade from realization. Ship designs, threats, tactics, and technology will continue to evolve over that time-frame, complicating concrete CONOPS discussions pertaining to an unknown futuristic maritime warfare environment. Therefore, this chapter will discuss CONOPS based on how the FEL may be used in the future as a point defense weapon system but modeled after tactics used on modern warships like the DDG-51 Class Arleigh Burke Guided Missile Destroyers. Basing CONOPS on a modern day platform allows today's warfighters to debate the issues with a sound foundation of tactical understanding and threat awareness.

B. SYSTEM INTEGRATION

1. General Characteristics

Before a discussion about FEL procedures and operations can commence, a few assumptions and characteristics will be defined. Future platforms will be constructed with the FEL in mind. Physical and engineering capabilities would be sufficient to support the operation of a single FEL system which would "feed" a number of topside beam directors. The actual arrangement of the directors, whether fore/aft, port/starboard, or a single director at the ships highest point, is inconsequential for this discussion, as long as 360º azimuth and 90º elevation coverage is achieved. Therefore, in the case of the CONOPS presented here, two such directors will be used, one forward and one aft, to provide 360º coverage with slightly overlapping amidships regions as shown in Figure 23.

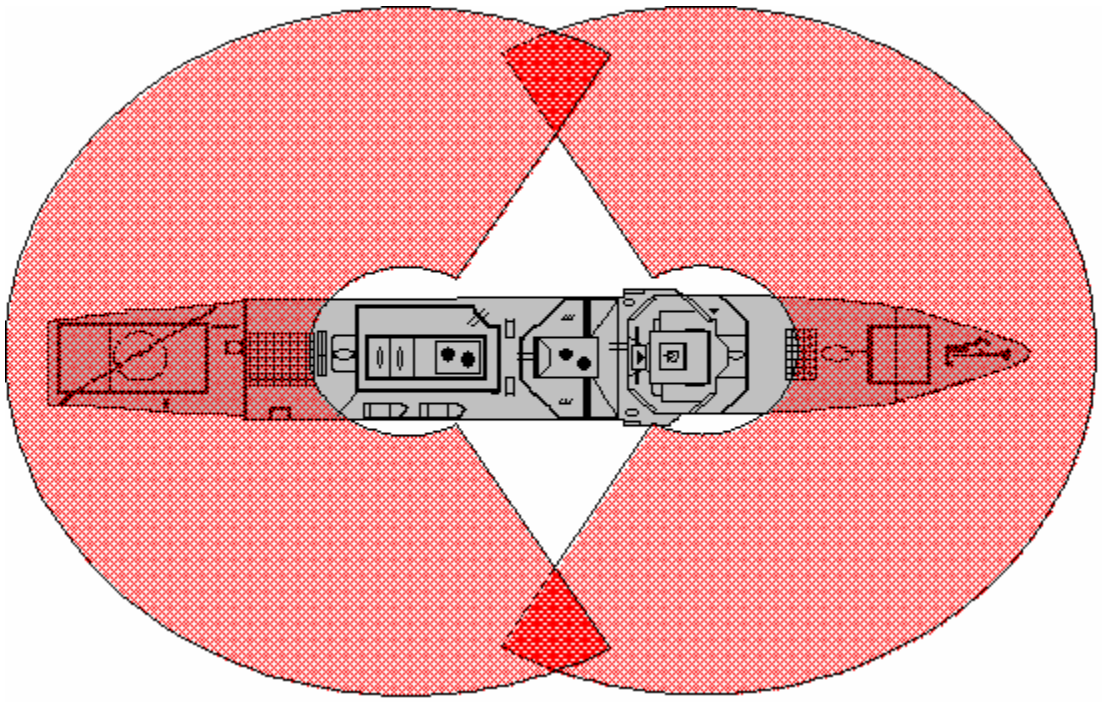

Figure 22. FEL 360º weapons coverage.

The range of any weapon system is always critical in determining appropriate CONOPS. Atmospherics and line-of-sight are the two major range limiting factors for any directed energy weapon. For the purposes of this chapter, the FEL's max range will be 5.5NM, with a nominal range of 2.7NM.

2. Mission

The primary mission for an FEL is ship self-defense, or point defense, as it is often called. Atmospheric effects on beam propagation in a maritime environment restrict an FEL's effectiveness as an extended range fleet defense weapon. As a point defense weapon, though, it is ideal, with its 360º coverage, speed of light delivery, deep magazine, and low cost per engagement. While anti-ship cruise missiles (ASCM) present the most prominent threat, asymmetric threats such as small boat attacks and low slow flyers (LSF-the terrorist's kamikaze), represent an emerging danger to naval platforms. The FEL as a point defense system is uniquely suited for this type of challenge, considering its flexibility and engagement options, which will be discussed later.

The Navy's increasing emphasis on littoral warfare necessitates a greater focus on Naval Surface Fire Support (NSFS). The FEL as an NSFS asset provides an engagement capability unheralded in the history of warfare. The nature of directed energy allows

precision engagements without the collateral damage associated with modern kinetic ordnance. FEL fire support can be directed at specific target sites despite highly sensitive surroundings. Power lines, communications equipment, sensor sites, artillery barrels, etc, represent only a portion of possible targets that may be engaged with directed energy. Engagements are not only possible against direct line-of-sight (LOS) targets, but also indirectly through the use of unmanned aerial vehicles (UAV) fitted with optical systems capable of receiving, redirecting and targeting ship-generated energy.

A third mission fitting within the FEL purview is anti-satellite warfare (ASAT). While the ranges are far greater than those suitable against low altitude threats, the lasing time may also be greater. A more diffuse beam would be used over a greater period of time as the target satellite traces an arc through the sky. The additive effect of the beam over time may cause sufficient damage to the sensitive satellite components to affect a soft kill.

3. Weapons Posture

Weapons postures designate weapon system readiness. They range from a level designed for maximum safety against an inadvertent firing to a level of maximum readiness for all weapon systems.

Weapons postures (WP) go from 1 to 4. WP 4 is the in-port state, where all systems are powered down, firing keys are locked in safes, and ammunition is downloaded. While systems may be powered-up temporarily for maintenance or training, all safeties will generally remain in place. WP 3 is the most secure at-sea state used during "peace-time" steaming. Under this posture both physical and electronic safety constraints are active, firing keys are removed from equipment but in the possession of warfighters, ammunition is uploaded, etc. The transition time from WP 4 to WP 3 can take hours and is generally initiated as part of an underway check-off list prior to heading out to sea. WP 2 takes one step closer to full combat readiness by removing physical safeties (electronic safeties remain active), and installing, but not turning, firing keys. The purpose of WP 2 is to remain in an alert status for extended periods of time as safely as possible. Transition from WP 3 to WP 2 ranges from 8-15 minutes depending on specific variations and requirements of each specific posture. WP 1 is the most combat ready state, all safety mechanisms have been removed from

weapons, permit switches are in the proper position, and firing keys are installed and turned. A ship at WP 1 is ready to engage any threat without weapon system readiness restraints. The time it takes to transition from WP 2 to WP 1 should only take a few seconds for a well trained combat team, allowing a ship to steam safety at the edge of complete readiness. While WP 3 and 2 can be maintained indefinitely, WP1 is typically only maintained for the duration of specific combat operation which can range from minutes to hours depending on the situation but never longer than necessary.

Weapons postures can be tailored for specific warfare areas, ie, air, subsurface, strike, and/or weapon systems, ie, vertical launch system (VLS), 5" Gun, etc. Therefore, if the ship is conducting tomahawk missions, it does not have to remove safeties for non-engaged warfare areas. Thus, weapons postures for the FEL would be independent of other weapon systems but may be escalated by its association with specific warfare areas.

Considering the missions that an FEL is capable of executing, it is logical for it to be part of both the air and surface warfare areas. An increase in the WP for either specific warfare area would mean increased readiness for the FEL and other associated weapon systems, ie VLS/SM-2 for in increase in Air related systems. For the FEL, WP transitions will involve changing engineering status and system safeties as depicted on the next page in Table 5. Actions that are bold denote modifications from the previous weapons posture. By the time WP 1 is achieved, the system is completely ready to engage targets at the push of a button.

Table 5 shows the general format used to guide watchstanders through the incremental steps required to either increase or decrease WP's. Every weapon and sensor system would have a similar table outlining engineering and safety readiness conditions. In this case, with WP 4 set, system readiness conditions would be establish as described under the status column. When ordered to transition to WP 3, watchstanders and technicians would run through the FEL WP Matrix to ensure all system components are adjusted to comply with WP 3 status. Once achieved, reports are made to the Tactical Action Officer that the increased readiness condition has been achieved. WP's are used for combat and combat training only. Separate procedures would be developed and utilized for maintenance and training to govern the status of FEL components.

FEL Weapon Posture Matrix

WP	Status	When	Duration	Transition
4	Eng: 1. Energy storage system de-energized. 2. High Power RF Fields off. 3. High Power Electron Beam off. 4. CIC FEL Console power off. 5. Director Optics off. 6. Director power off. 7. Resonator Cavity Stability System off. Safety: 1. Drive Laser cutoff enabled (local) 2. RF Field cutoff enabled (key in safe) 3. Director depermit. (console push button). 4. Director shutter locked. (key in safe).	In-port	Indefinite	4→3 (hours)
3	Eng: 1. Energy storage system de-energized. 2. High Power RF Fields off. 3. High Power Electron Beam off. 4. CIC FEL Console power **on**. 5. Director Optics **on.** 6. Director power off. 7. Resonator Cavity Stability System **on.** Safety: 1. Drive Laser cutoff enabled **(remote).** 2. RF Field cutoff enabled **(key with TAO)** 3. Director depermit. (console push button). 4. Director shutter locked. **(key with AIR)**	Peacetime Steaming	Indefinite	3→2 (mins)
2	Eng: 1. Energy storage system **energized.** 2. High Power RF Fields off. 3. High Power Electron Beam off. 4. CIC FEL Console power on. 5. Director Optics on. 6. Director power **on.** 7. Resonator Cavity Stability System on. Safety: 1. Drive Laser cutoff **disabled** (remote). 2. RF Field cutoff enabled **(key inserted).** 3. Director **permit** (console push button). 4. Director shutter **unlocked.**	Alert	Indefinite	2→1 (secs)
1	Eng: 1. Energy storage system energized. 2. High Power RF Fields **on**. 3. High Power Electron Beam off **(*)**. 4. CIC FEL Console power on. 5. Director Optics on. 6. Director power on. 7. Resonator Cavity Stability System on. Safety: 1. Drive Laser cutoff disabled (remote). 2. RF Field cutoff enabled **(key engaged).** 3. Director permit (console push button). 4. Director shutter unlocked.	Combat	As required by tactical situation	

(*) Depression of the "lase" button on DEWS console will activate the drive laser which will stimulate the ejection of electrons off of the photocathode to generate the electron beam.

Table 5 Weapons Postures for an FEL.

a. Safety Mechanisms

Safeties are a critical component of the FEL design and weapons posture matrix. Safeties are purposely redundant and dispersed to various ship locations and different watchstanders so as to ensure no one person can easily take control of the entire system. Table 5 catalogs four different safety mechanisms designed to prevent damage to personnel and equipment, and to prevent the inadvertent "firing" of the system.

The first safety involves the Drive Laser Cutoff (DLC) which has two positions, either enabled or disabled, and two control options, local and remote. When the DLC is enabled, the electricity required to power the drive laser is physically interrupted by a push button switch. When it is disabled, the circuit is completed and power will be provided to the laser. The local and remote positions are utilized primarily for maintenance and underway operational control. When in local, the technicians at the FEL have control of the DLC. When in remote, the Combat Information Center (CIC) watchstanders have control of the DLC. It is important to understand the distinction that disabling the DLC does not mean that the drive laser is lasing. The drive laser only lases either for maintenance or when engaging a target.

The second safety is the RF Field Cutoff (RFFC) which has the same enable and disable positions as the DLC. When enabled, the RF fields in the accelerator and the photoinjector are not energized, prohibiting the electron beam from being accelerated. When disabled, the RF fields are fully energized. Since the RF fields are the major limiting factor concerning system availability, primarily due to cooling issues, the RFFC can only be controlled from CIC with a key. When in-port, the key is locked in the Commanding Officers safe, but while underway, the key is maintained by the Tactical Action Officer, or TAO, the most senior CIC watchstander. The TAO will then use the key as directed by the weapons posture matrix.

The next safety is the Director permit. This safety creates an electronic interlock which either allows or prohibits the director from slewing away from the storage position. When permitted, the director may train in any direction limited only by the physical cutout stops which keep the FEL from lasing back into the ship. Depermitting the director would keep it from slewing onto a target. This safety involves

nothing more than a push button on the Directed Energy Weapons Supervisor (DEWS) console but it provides one more "man in the loop" to ensure safety.

The final safety mechanism is a physical restraint which locks the director protective shutter. To unlock the shutter, an FEL technician will have to physically go out to the director and remove the locking device. This safety does not necessarily prohibit the system from firing but instead serves as an additional measure to protect the highly sensitive outer director lens.

4. Watchstanders

The FEL will be operated from CIC by a watchstander called the Directed Energy Weapon Supervisor (DEWS). The DEWS will be a subordinate watchstander position under the management of the Air Warfare Coordinator (AIR) who answers directly to the Tactical Action Officer (TAO) or the Commanding Officer (CO) if present. The relationship between the AIR and DEWS will be similar to that between AIR and the Missile System Supervisor (MSS). AIR manages the air "picture" and passes "kill" orders to MSS, or in this case DEWS, for engagement by their specific weapon system. A detailed CIC watchstander organizational diagram including the DEWS is depicted in Figure 24.

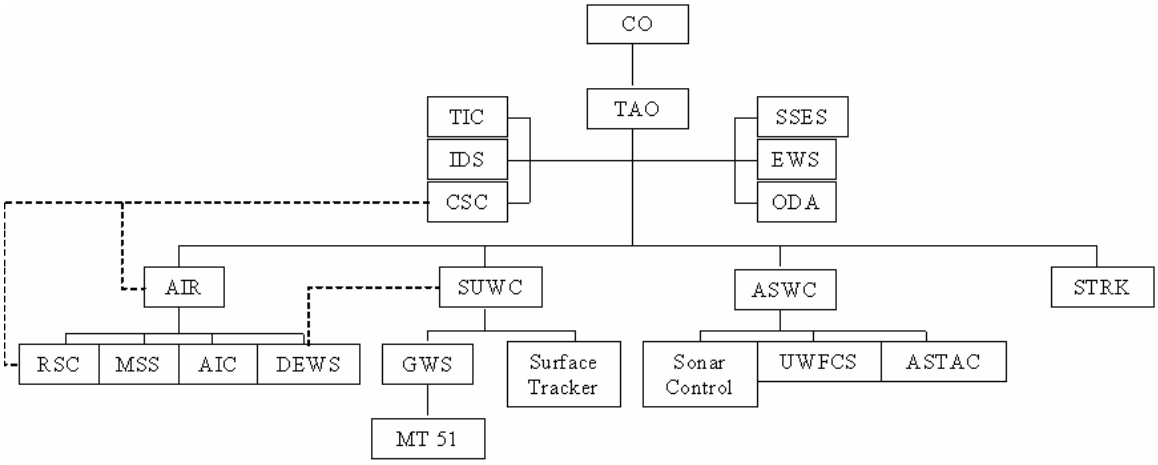

Figure 23. Combat Information Center Organization with Directed Energy Weapons Supervisor included.

While the FEL would be under the primary ownership of AIR, control must be relinquished to the Surface Warfare Coordinator (SUWC) for FEL surface engagements.

In instances where there may be a conflict between air and surface engagement priorities, the TAO will decide which threat is the most critical.

DEWS watchstanders will be drawn from the same personnel responsible for the systems maintenance. Fire Controlmen (FC) are the most logical choice for this task. Already responsible for numerous sensor and weapon systems onboard modern naval platforms, the FEL FC's will received specialized training and be awarded a directed energy Naval Education Code (NEC) for FEL maintenance and operation, tagging them as system experts. In addition to FEL maintenance and watchstanding responsibilities, FEL coded FC's will be required to take atmospheric measurements prior to assuming each watch in an effort to determine the "range of the watch." Similar to the Sonar Technicians (ST) measuring salinity and temperature profiles to determine an acoustic "range of the day," the FC's "range of the watch" will allow AIR and the TAO to make critical tactical decisions based on predicted optical beam propagation ranges.

Modern naval combat is managed by a philosophy of command-by-negation, where warfare coordinators conduct operations within their specific areas of responsibility until their actions are "checked" by their superiors. On individual ships, the most senior watchstander in CIC is the TAO or the CO who oversee combat operations from consoles which can monitor the entire battlespace on large screen displays, Figure 25.

Figure 24. Commanding Officer and Tactical Action Officer Console in DDG 51 Class Guided Missile Destoryers.

An FEL engagement would follow the same philosophy. AIR would order DEWS to engage a specific track and it would be up to the TAO or CO to retract that order if they determine that the engagement is not warranted. Engagement options and specific tactics will be covered in Sections C and D.

5. Detect to Engage Sequence

The Detect to Engage (DTE) sequence is a tool utilized to help warfighters learn, understand, and put into practice the concept of layered defense, or defense in depth. DTE is a sequential listing of detection and engagement ranges, from maximum to minimum, of all of a platform's sensors and weapons systems. Arrayed in this manner, warfighters quickly learn to identify sensor and weapons system overlap regions, and more importantly, how many "chances" a ship might have at engaging a particular threat from the time it is detected to the time it closes within a ship's minimum engagement range.

Figure 26 depicts a rough DTE schematic including the hypothetical ranges for the proposed FEL system. Specific ranges and entire sensor systems (ie SLQ-32) are purposely omitted in order to maintain an unclassified thesis. The benefits to this figure are that it shows the integration and basic overlap regions the FEL would share with other weapon systems on the same platform.

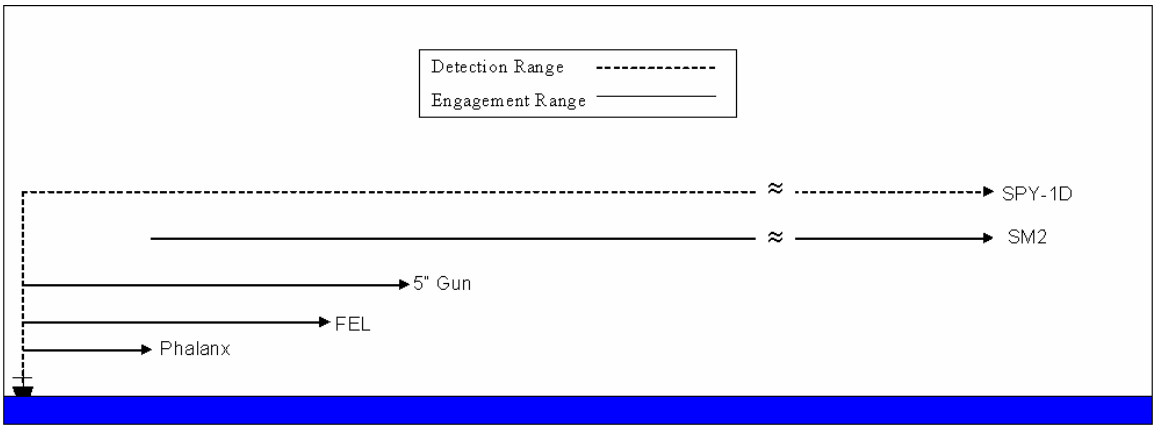

Figure 25. DTE with incorporated FEL weapon system.

Note specifically that the ranges for SPY-1D and the Standard Missile (SM) 2 are not to relative scale since the advertised unclassified detection range for the Aegis system is 200+ NM which is target attitude dependent.

C. ENGAGEMENT OPTIONS

For nearly every weapon system onboard Navy surface combatants there are two options by which a target can be engaged, either manually or through some automatic process. The FEL would be no different. Embracing both engagement options as a matter of practice allows the FEL to confront a wide spectrum of threats from highly agile, supersonic ASCM's to much slower surface craft.

1. Detection, Tracking, and Fire Control

In order for a threat to be engaged, it must first be detected, tracked, and identified as a threat. The threat "track" can then be passed to a specific weapon system which will continue to track the threat and eventually engage it through a fire control process.

The detection and tracking of contacts would be conducted via an organic volume search radar (VSR) system like the SPY-1D radar, with the exception of subsurface contacts. Once a contact has been detected and is being tracked, it is displayed to watchstanders on CIC consoles as a "track." A complex systems of symbols allow watchstanders to distinguish air tracks from surface tracks, friendly tracks from unknown tracks, etc. Subsurface tracks, while not detected by a standard volume search system, are displayed on the consoles in CIC for all watchstanders to view. Identifying tracks as either friendly, unknown, neutral, suspect or hostile is done manually through a combination of intelligence, situational awareness, visual identification (typically by aircraft), and standard rules of engagement (ROE).

Threat tracks receive extra attention by both system resources and watchstanders. Once the determination has been made for a track to be engaged, a weapon system(s) is selected to conduct the engagement, and the track information (bearing, range, altitude, speed, target angle, etc) is passed to the selected system for fire control. Fire control is the process of tracking the target just prior to and throughout the duration of the engagement, and the pointing of the weapon system in the direction of the inbound target. Beam control which involves optical beam target focusing, atmospheric compensation, and lase-time requirements is contained within the fire control process.

In regards to FEL fire control, track information would be passed to the FEL fire control system (FCS) in order to provide a "general area" where the system should "look" for the target. The FEL FCS will then use a series of organic passive trackers to search

for and then refine target resolution and magnification. Laser illuminators help to define the target's shape in order to drive the beacon laser onto the target, which is used for aimpoint selection and atmospheric compensation. Once the beacon laser is locked onto the proper aimpoint, the target can then be engaged. This entire process only takes a fraction of a second.

Battle damage assessment (BDA) is the process by which a determination is made whether or not the engagement had the desired effect against the intended target. BDA for FEL engagements could possible come from a combination of two sources. The first method would be through watchstander visual confirmation through the FEL's organic laser/optical search and track system. The second method would stem from the ships VSR which would input a targets post-engagement differential speed, altitude, and surrounding track starts into an algorithm to determine if the engagement was successful.

The FEL director is essentially a big telescope and therefore could be used as a long range surveillance, identification, and tracking asset without the generation of an optical beam. ROE issues pertaining to this method of use would reside with the CO.

2. Manual Engagements

Manual engagements are those which require direct watchstander action to lase a target. Tracks can either be engaged by watchstanders "hooking a track" (selecting a track with a point and click mouse like cursor) and depressing the engage Variable Action Button (VAB) or by visually locking onto a contact through the FEL FCS laser/optical system for a Manually Observed Visual Engagement, or MOVE.

The hooked track engagement method is traditionally the most common engagement method. It allows watchstanders to quickly identify hostile threats, rapidly retarget and engage them without the time consuming process of visually identifying targets. Unfortunately this method would not permit manual aimpoint management which is permitted in a MOVE engagement. Through this method, tracks can be engaged whether or not they are within FEL range. Tracks which are out of range will be placed in an "engagement queue," which allows the system to automatically engage the track when it has achieved engagement criteria. An automatic BDA calculation will determine dwell time. For example, AIR orders DEWS to engage an inbound ASCM at 10NM. DEWS hooks the track and depresses the engage VAB on his/her console which orders

the VSR to pass targeting information to FEL FCS. Since the target is out of range, the engagement order is placed in the engagement queue, waiting for the target to come within 5.5NM. Once the proper criteria have been met, FCS will order the director to slew onto the correct bearing and elevation to consummate the engagement. Tracks which are within FEL range will be immediately engaged unless there are higher priority FEL engagements being conducted, in which case they too would be placed into the engagement queue.

A MOVE engagement would allows watchstanders to visually observe a target through the FEL FCS laser/optical system through a monitor mounted near the DEWS console. DEWS can either use a joystick device to manually scan for a contact or he/she can slave the FCS laser/optical system to point at a contact which is hooked. Once a contact is within visual range on the optical system, DEWS can fine tune the aimpoint through manual control of the beacon laser (ie, onto the engine block of a small boat) and consummate the engagement. The FEL will dwell as long as the "fire" button is depressed. There are a number of advantages and disadvantages to this manner of engagement. MOVE allows watchstanders to personally identify contacts before engaging them and allows for pinpoint engagement accuracy against larger slower moving contacts. It is also critical for proportional engagements which will be discussed in Subsection 4. The major disadvantage is that it is a very time consuming process. The speed of naval warfare may not permit such engagements when seconds are critical. It would be up to the discretion of the CO as to when MOVE engagements would be permitted.

3. Automatic Engagements

Similar to the Aegis Weapon System (AWS), future combat systems will have the capability to automate a number of functions in order to reduce the watchstander workload allowing them more time to concentrate on combat situational awareness. It can even automatically engage threat tracks if the ship's safety is deemed to be in extremis. These automated actions would be accomplished through "doctrine statements." Doctrine statements can be view as small computer programs created by ships-force personnel which command the combat system to perform specific operations.

Track identification, track load reduction, alerts, and specific engagements can all be automated through the use of doctrine.

Specialized "engagement" doctrine can be written to automate the FEL engagement process. The primary intent of this type of doctrine would be as a last ditch defensive effort to protect the ship from "leakers," or tracks which have slipped through other ship defenses. As beneficial as this may be, it must be carefully monitored to ensure unintended tracks do not get engaged, therefore doctrine parameters must be restrictive by nature. Such constraints to engagement doctrine could be, but not restricted to, engaging only inbound non-friendly (not hostile tracks only) air tracks within 5NM. With these constraints, FEL engagement doctrine, when active, will not engage crossing, outbound and/or surface tracks. The authority to activate such doctrine is held by the CO and the TAO.

4. Proportional Engagements

Unlike conventional kinetic ordnance, an FEL has the functionality to tailor the energy imparted on the target. This unique capability allows the FEL to conduct proportional engagements, from low power "warnings" to high power hard kills.

In order to change the optical beam's output power, the undulator would have to be supplied with a variable power electron beam from photoinjector. By rapidly switching off and on the photoinjector drive laser on a millisecond time-scale the average power can be arbitrarily adjusted. For operational simplicity sake, it is foreseeable that there would be two or more FEL settings available to watchstanders, from a high power hard kill setting to a low power illumination setting.

The high power setting would be utilized for missions such as NSFS, ASAT, and point defense against ASCM's and other critical hard kill targets. At the flip of a switch, DEWS would be able to transition to low power mode, allowing the ship to shoot the proverbial "shot across the bow," or to intentionally warn potential adversary's by blistering paint, personnel, or other equipment. Aimpoint selection is extremely important for a low power illumination to be effective; therefore this method of engagement would only be available through a MOVE. Proportional engagements also provide the CO with greater options during questionable rules of engagement scenarios.

D. TACTICS

Tactics are the methods by which a ship fights, balancing firepower, mobility, radar cross section, engagement options and mission requirements against anticipated threats. Tactics would be different depending on whether the FEL is being used in a point defense role or for an NSFS role. Matching engagement options to specific threats falls within the realm of tactics.

1. Point Defense

Point defense is the primary mission of the FEL and encompasses a wide spectrum of possible threat tracks. Point defense (PD) engagements will normally be against high speed ASCM threats but also slower surface or LSF contacts. Regardless, this manner of engagement requires a manual hooked track with high power lasing to eliminate the threat and rapidly retarget. A "kill" order by AIR to DEWS will initiate the process to conduct a high power engagement against the assigned track. MOVE engagements for PD will have to be specifically ordered by the TAO and will normally be reserved for surfaces and/or LSF threats where greater reaction time available.

2. Naval Surface Fire Support

Naval Surface Fire Support (NSFS) is considered an offensive capability and therefore must be performed in the presence of the CO. NSFS can be conducted either against direct line-of-sight (LOS) targets, or indirectly through the use of unmanned aerial vehicles (UAV).

For LOS NSFS engagements, the ship will have to be within approximately 5 NM of the intended target. Either a shore based target designator laser or the FEL beacon laser will have to "paint" the target for fire and beam control. Dwell time will be determined either by the unit calling for fire or optically by ship's-force personnel.

It is proposed that UAV's fitted with optical systems capable of receiving, redirecting and targeting ship-generated energy will be controlled by shore-based surface fire support teams. When an indirect fire support mission is called in to the ship, target coordinates are sent to the ship to determine the optimum UAV position for beam redirection. Just prior to the engagement, the ship will take automated control of the UAV to fly it to the required bearing, range, altitude, speed, and target angle. Once in the

position, the UAV's beacon laser will be used as the FEL's aimpoint to ensure the ship-generated optical beam is properly received. Dwell time will be determined by the unit calling in the fire mission.

3. Anti-Satellite (ASAT)

ASAT engagements will as well require direct participation from the Commanding Officer and would be conducted much like modern Tomahawk missions. Stateside-based engagement planners would determine all required details for the ASAT mission, including ship's position and heading, laser power and dwell time, azimuth, elevation and slew rate. This information is passed to the ship via encrypted satellite data link and directly fed into the FEL FCS for final ship-directed engagement planning. It would be up to the ship's crew to ensure the ship is in the proper location and the laser is in the proper configuration in order to successfully conduct the mission. At the prescribed time, ships-force personnel will initiate the engagement and allow the FEL FCS to automate the remainder of the longer than average lase time.

4. Guarded Unit State

Atmospheric propagation effects do not provide sufficient range for an FEL to provide theater coverage, but it can be used as a limited area defense weapon system under the proper conditions. As an area defense weapon system, an FEL may be able to defend one or two other surface vessels which are steaming in close formation with the FEL platform. Such circumstances such as underway replenishment (UNREP), plane guard, and/or amphibious operations could provide close enough ship formations to fall under the umbrella of FEL area coverage.

It is estimated that up to two vessels may be placed under the protection of the FEL through the Guarded Unit State (GUS) function operated by the DEWS. GUS has to be operated in conjunction with FEL auto-engage doctrine. When GUS is operating, the FEL FCS will engage not only tracks threatening ownship, but also those that are targeting the guarded units. A threat priority matrix will determine which tracks are engaged in what order but the system will always default to protect itself if the engagement queue becomes saturated.

Since GUS engagements would be "seen" as crossing targets to the FEL FCS, the optical beam would be propagating through an ever changing air column, leading to

reduced atmospheric effects and therefore slightly increased range. As a result, guarded units may skirt the maximum range of the FEL and still be protected. Admittedly, the closer to the FEL platform the better, but ship navigation safety must be the over-riding consideration.

E. CONOPS SCENARIO (STREAM RAID)

The development of a CONOPS scenario helps to showcase the FEL as a weapon system in a tactical situation which it may be employed in the future. Such scenarios are often used as training tools for ship crews to help sharpen their combat effectiveness, system understanding, and situational awareness.

This particular scenario takes place in the Arabian Gulf in the near future.

1. Geopolitical Situation

Continued unrest in Iraq following the Second Gulf War has caused a sharp rise in anti-American sentiment amongst Arabs throughout the world and particularly in the Arabian Gulf region. While Arab state leaders pledge support for the United Nations (UN) sponsored Iraq reconstruction plan, they have failed to curtail escalating inflammatory rhetoric amongst Muslim clerics and militant radicals.

Last week, the USS OSCAR AUSTIN intercepted a dhow, Figure 27, in the South Arabian Gulf (SAG) while conducting routine Maritime Interception Operations (MIO). After a quick inspection of the cargo hold and navigational charts, it was determined that the dhow was smuggling SS-N-22 "Sunburn" cruise missile guidance components from an undisclosed port of origin toward the Strait of Hormuz. Interrogations later revealed that the smugglers were members of an Al-Qaeda sponsored terrorist organization striving to "rid Arabian Gulf waters of the American pestilence."

All U.S. warships in the Arabian Gulf are ordered to remain especially vigilant for small boat attacks and possible rouge cruise missile launches against U.S. and/or international shipping. Top secret negotiations are underway in the UN to affect a shipping escort plan in an effort to protect all shipping in and out of the Gulf.

Figure 26. Dhow intercepted by USS OSCAR AUSTIN (DDG 79)

2. Event Timeline

On 4 November, the USS RESONATOR (DDG-22), a new FEL equipped Zumwalt-Class Guided Missile Destroyer, is transiting from the North Arabian Gulf (NAG) to Abu Dhaby, UAE for a port visit. Communication intercepts from RESONATOR's embedded Signal Exploitation detachment indicate chatter between an unidentified shore installation and a waterborne craft. The exact nature of the communiqué is unclear but it appears to be bearing and range estimations. Coordination with an orbiting EP-3 has triangulated the shore installation to be on either Bani Forur Island or Siri Island, Figure 28. Quick calculations by the TAO suggest that the bearing and range measurements are those of the RESONATOR to the vicinity of the islands. The TAO immediately calls the CO to CIC and increases the WP from 3 to 2. RESONATOR is currently on a heading of 135º at a speed of 15kts, approximately 50 miles Southwest of Siri Island and 37 miles Northwest of Sir Abu-Nu'ayr Island.

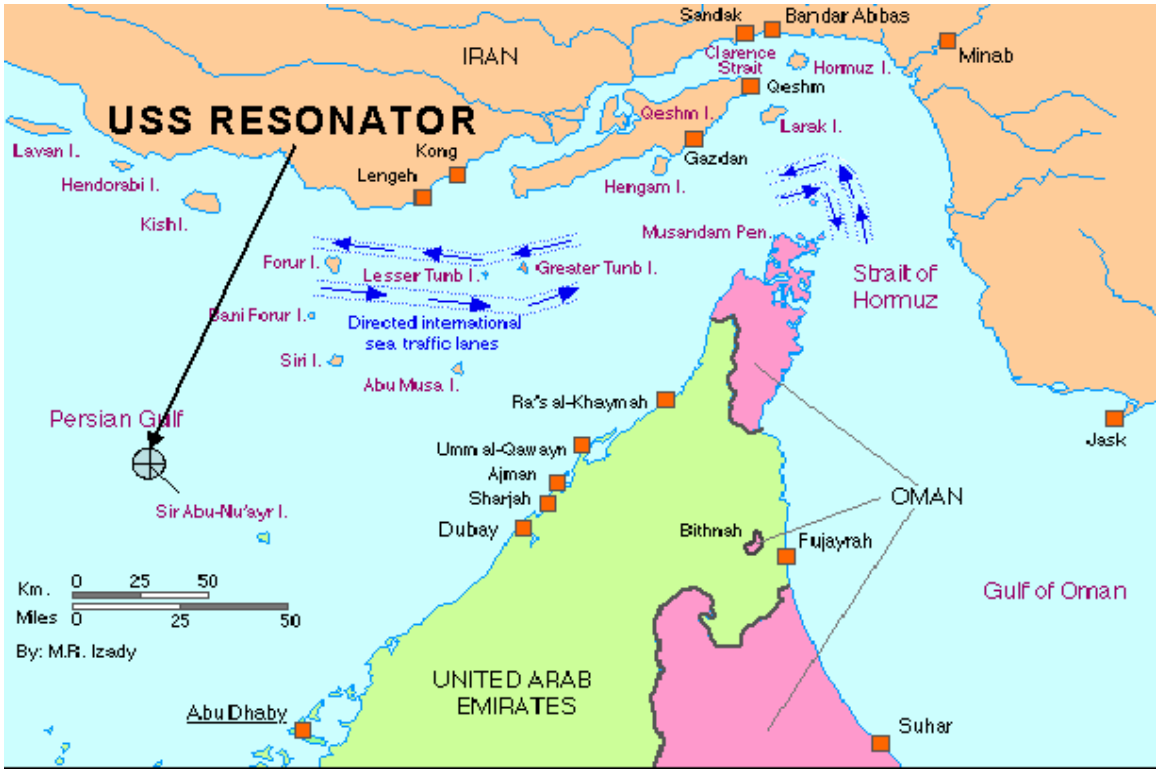

Figure 27. Strait of Hormuz and South Arabian Gulf.

Time 00:00:00 (Scenario start time). Ships Signal Exploitation Space (SSES) personnel notify CIC that RESONATOR may be being located and targeted utilizing geographic references. The TAO immediately calls the CO to CIC and increases the ship's WP from 3 to 2.

Time 00:01:00 (1 minute into scenario). The CO arrives in CIC and assumes the watch. RESONATOR maintains course and speed.

Time 00:03:00. SSES reports additional chatter between the shore installation and waterborne craft. Translations suggest the shore installation is ordering the targeting craft to clear the area. Bridge personnel report trailing dhow changing course to open the distance between themselves and the RESONATOR. CO orders WP 1 set.

Time 00:07:30. All stations report WP 1 set.

Time 00:08:00. AIR reports, "Vampire, Vampire, Vampire, bearing 049°, range 50 miles, composition 5." The RESONATOR's VSR holds the tracks temporarily as they climb through boost phase, Figure 29, but then loses track as they dip back down into their sea-skimming cruise phase.

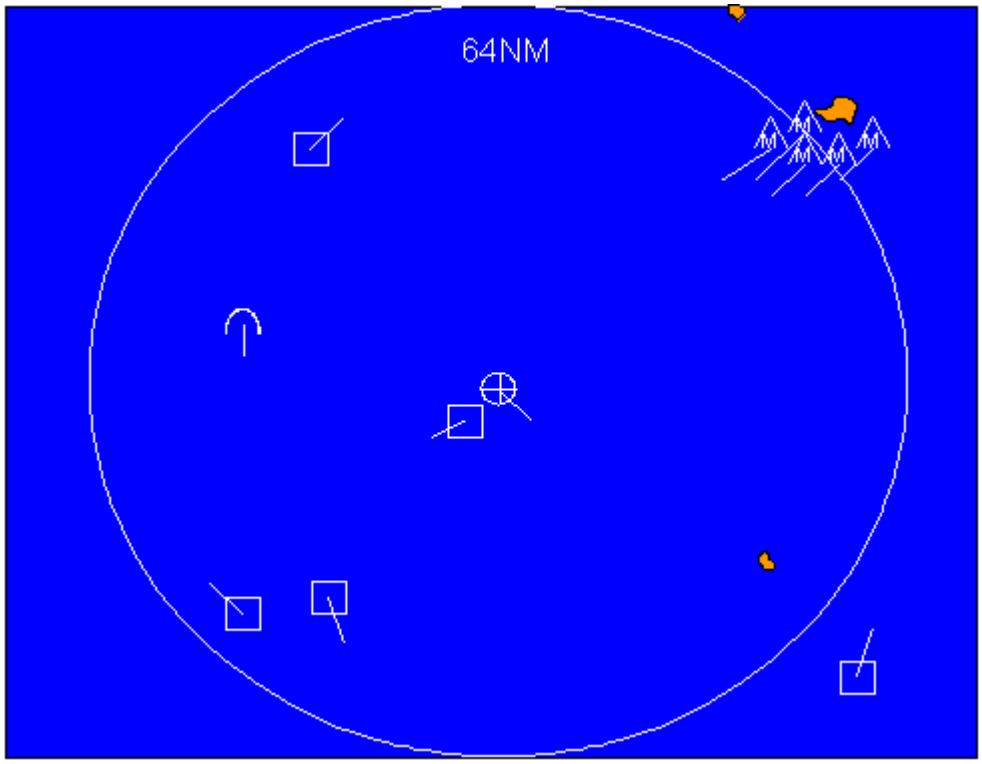

Figure 28. Console view of tactical situation at Time 00:08:00. RESONATOR's VSR has detected missile launches from Siri Island.

Time 00:08:02. The CO orders auto engagement doctrine set for SM-2 and FEL, and sets General Quarters to prepare the ship for damage control.

Time 00:09:36. The VSR requires the inbound missiles at approximately 12 NM from RESONATOR. The Auto engagement doctrine is automatically tripped, triggering a volley of missiles to erupt from their VLS cells and race toward the inbound threats, Figure 30.

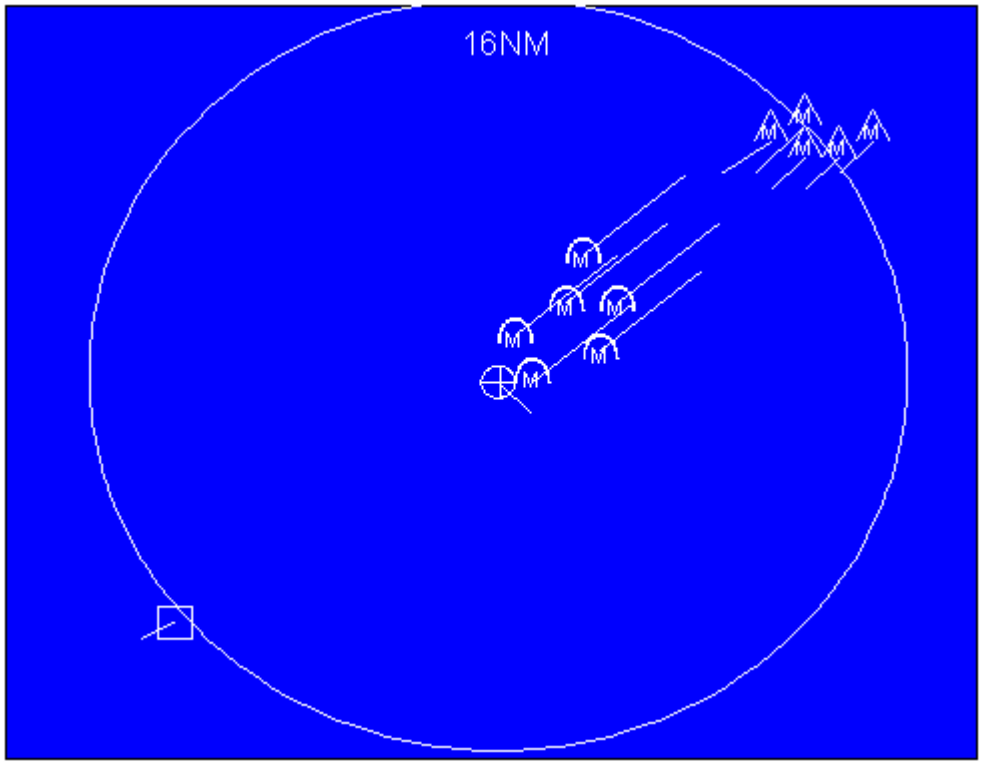

Figure 29. Console view of tactical situation at Time 00:09:36. Auto engagement doctrine has automatically engaged the inbound threats. Note the range change from 64 NM to 16 NM.

Time 00:09:44. First volley of SM-2's reach target intercept point and destroy 3 of 5 inbound threats at a range of approximately 8.5 NM. The two remaining threat tracks continue inbound.

Time 00:09:47. The VSR calculates that the next possible SM-2 engagement is within the minimum missile engagement range and orders the FEL to slew onto the threat bearing.

Time 00:09:49. Both FEL directors slew onto their assigned targets while the FEL FCS determines which of the threats to engage first.

Time 00:09:51. Director 1 (forward director) unleashes a multi-megawatt optical beam at the nose cone of the first inbound leaker at a range of 5.5 NM, Figure 31, and dwells for 3 seconds effecting a hard kill at 4.3 NM

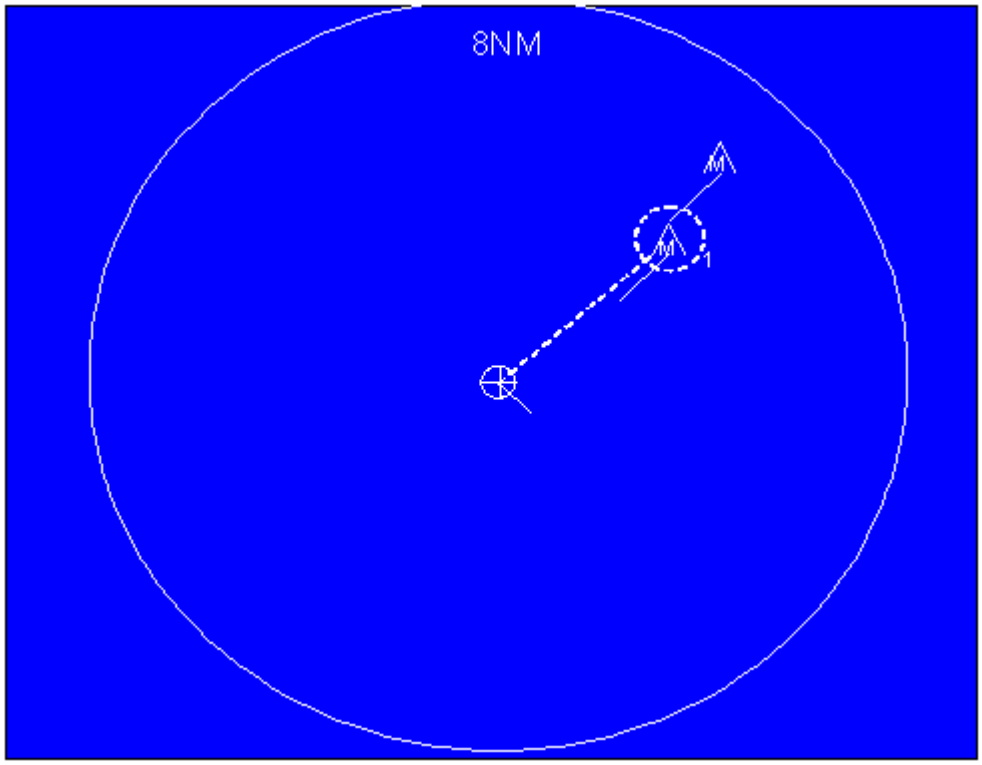

Figure 30. Console view of the tactical situation at Time 00:09:51. FEL Director 1 engages the first inbound leaker. Note the range change from 16 NM to 8 NM

Time 00:09:55. The optical beam is transitioned to director 2 (aft director) to engage the second leaker at a range of 3.9 NM. 3 seconds later the second threat track is splashed at a range of 2.6 NM.

Time 00:10:00. The TAO reports to BZ that all vampires have been splashed.

Time 00:10:30. BZ orders RESONATOR to intercept and detain the crew of the suspected targeting vessel. RESONATOR immediately alters course to 225º and increases speed to 30+kts.

Time 00:31:00. RESONATOR approaches within 2 miles of the dhow suspected of providing targeting information for the ASCM attack. Repeated radio request to stop and prepare to be boarded have been met by silence from the dhow's crew. BZ authorizes the use of force to detain the vessel and crew.

Time 00:31:05. SUWC takes control of the FEL and orders DEWS to perform a high power MOVE on the stern engine compartment of the dhow for 5 seconds.

Time 00:31:07. DEWS selects the MOVE option and utilizes a crosshair and joystick assembly to target the dhows engine compartment on the console monitor. DEWS then verifies the engagement order and depresses the "lase" button for an audible 5 count.

Time 00:31:12. Cease fire. Billowing black smoke shrouds the stern of the dhow as it slowly reduces way and comes to a relative halt. Crew members are visible on the monitor attempting to extinguish growing flames and waving to RESONATOR in surrender.

Time 00:35:00. RESONATOR's boarding team is dispatched to board and detain the crew of the dhow.

3. Conclusion

While this scenario is simplistic in nature it demonstrates a number of valuable considerations. First, that the FEL is primarily a point defense weapon, utilizing speed and lethality to successfully engage multiple leaker threats. The FEL easily filled the gap once the threat track closed within the minimum missile engagement range.

Additionally, the FEL was used in a non-lethal surface action to enforce the direction of higher authority. Disabling the dhow's engine without the expected collateral damage associated with a kinetic weapon system allowed the boarding team to successfully apprehend the dhow's crew without unnecessary casualties.

While this scenario demonstrated only a portion of the FEL utility, it provided a realistic example of possible employment applications in real time, distances, and speeds.

VII. CONCLUSION

The U.S. Navy's vision for next-generation weapon systems includes the use of an FEL as a point defense weapon system, which promises significant tactical advantages over current weapon systems. The speed of light delivery of MW+ power will be sufficient to kill modern and emerging threats, while the advantages of low cost, multi-mission capabilities, and a near limitless magazine will place it on the forefront of shipboard design consideration.

At the Naval Postgraduate School, a high power FEL design is being designed to meet the Navy's needs. In order to produce a ship-worthy system, a short Rayleigh length design has been proposed to eliminate the critical issue of resonator mirror intensity damage. Such a system will allow a shorter resonator cavity, resulting in a more compact system for shipboard integration. A possible disadvantage of such a design is that a slight electron beam misalignment through either offset or tilt may cause a reduction in the overlap between the electrons and the small optical mode waist, resulting in less gain and extraction. Three-dimensional computer simulations were used to determine whether vibrational effects can change the optical wavelength and unexpectedly reduce the extraction as the electron beam is offset further from the undulator axis. Results showed that the extraction required for a MW of output power is achieved for electron beam shifts of as much as 0.3 mm, which is much bigger than the achievable experimental design tolerances of 0.01 mm, so that this is not a problem. Also demonstrated were the effects of electron beam focusing on extraction. It was shown that the focusing enhanced the overlap region between the electron beam and the optical mode, resulting in an increase in extraction efficiency far beyond the required values. Such results prove that it may be possible to obtain a MW of power at a lower average current.

High power resonator cavity parameters, namely the number of undulator periods, the electron beam radius, and the Rayleigh length, were also studied to determine their optimal values. While specific numerical values were determined, the greatest benefit of this research stems from the understanding of the relationships between FEL parameters. Specific values describing the FEL may change as parameters are scaled to meet MW-

class requirements, but underlying trends and concepts will probably remain the same, leading to a greater overall understanding of the design issues.

The Concept of Operations developed in this thesis is simply a stepping stone to improve system capability awareness and tactical utility. It serves as a launching point for future discussions concerning exactly how FEL doctrine should be developed in order to maximize system performance, integration and functionality.

Continued funding and research are crucial in order to bring the FEL to the fleet. There are many advantages of such a system and these will only be realized through the maintenance of the vision of revolutionizing the maritime battlefield by the use of directed energy.

LIST OF REFERENCES

[1] Email between George R. Neil, Thomas Jefferson National Laboratory and the author, 25 February 2003.

[2] Email between Alan M. M. Todd, Advanced Energy Systems, and the author, 13 February 2003.

[3] David J. Griffiths, "Introduction to Electrodynamics – 3rd Edition," 1999, Prentice Hall, Upper Saddle River, NJ.

[4] T. Campbell, "Simulations of a Short Rayleigh Length 100kW Free Electron Laser and Mirror Stability Analysis," Master's Thesis, December 2002.

[5] W.B. Colson, in: W.B. Colson, C. Pelligrini, A. Renieri (Eds) *Laser Handbook*, Vol.6., Chapter 5, Elsevier Science Publishing Co., Inc., The Netherlands, 1990

[6] W.B. Colson, A.M. Todd, and G.R. Neil, "Free Electron Laser with a Short Rayleigh Length," Nucl. Instr and Methods, A483, pp II-9 (2002)

[7] J. Blau, V. Bouras, A. Kalfoutzos, G. Allgaier, T. Fontana, P.P. Crooker, and W.B. Colson, "Simulations of High Power Free Electron Lasers with Strongly Focused Electron and Optical Beams," Nucl. Instr and Methods, A507, pp 44-47, (2003)

[8] J. Blau, G. Allgaier, S. Miller, T. Fontana, E. Mitchell, B. Williams, P.P. Crooker, and W.B. Colson, "Multimode Simulations of a Short-Rayleigh Length Free Electron Laser," Submitted at International Free Electron Laser Conference in Tsukuba, Japan, 2003.

[9] A. Kalfoutzos, "Free Electron and Solid State Laser Development for Naval Directed Energy," Master's Thesis, December 2002.

[10] V. Bouras, "High Energy Lasers for Ship-Defense and Maritime Propagation," Master's Thesis, December 2002.

[11] R.D. McGinnis, “High Energy Laser Efforts,” PMS 405 Presentation, NPS, March 2002.

[12] W.B. Colson, “Free Electron Laser Analysis, Modeling and Simulation,” Presentation, NPS, June 2002.

INITIAL DISTRIBUTION LIST

1. Defense Technical Information Center
   Ft. Belvoir, Virginia

2. Dudley Knox Library
   Naval Postgraduate School
   Monterey, California

3. Professor William B. Colson, Code PHCW
   Department of Physics
   Monterey, California

4. Professor Joseph Blau, Code PHBL
   Department of Physics
   Monterey, California

5. Professor Peter Crooker, Code PHCP
   Department of Physics
   Monterey, California

6. Professor Robert L. Armstead, Code PHAR
   Department of Physics
   Monterey, California

7. Chairman, Physics Department, Code PHMW
   Naval Postgraduate School
   Monterey, California

8. Engineering and Technology Curricular Office (Code 34)
   Naval Postgraduate School
   Monterey, California

9. CAPT Roger McGinnis, USN
   Naval Sea Systems Command
   Washington D.C.

10. Dr. George Niel
    TJNAF
    Newport News, Virginia

11. Dr. Steve Benson
    TJNAF/MS6A
    Newport News, Virginia

12. Dr. Fred Dylla
TJNAF
Newport News, Virginia

13. Dr. Alan Todd
Advanced Energy Systems
Princeton, New Jersey

14. LT Timothy S. Fontana
Surface Warfare Officers School, Department Head School
Newport, Rhode Island